Contrib Mineral Petrol (2003) 144: 570–591
DOI 10.1007/s00410-002-0416-z

ORIGINAL PAPER

Michael G. Davis · Michael O. Garcia · Paul Wallace

Volatiles in glasses from Mauna Loa Volcano, Hawai'i: implications for magma degassing and contamination, and growth of Hawaiian volcanoes

Received: 24 November 2001 / Accepted: 28 August 2002 / Published online: 7 November 2002

Abstract Glasses from Mauna Loa pillow basalts, recent subaerial vents, and inclusions in olivine were analyzed for S, Cl, F, and major elements by electron microprobe. Select submarine glasses were also analyzed for H_2O and CO_2 by infrared spectroscopy. The compositional variation of these tholeiitic glasses is dominantly controlled by crystal fractionation and they indicate quenching temperatures of 1,115–1,196 °C. Submarine rift zone glasses have higher volatile abundances (except F) than nearly all other submarine and subaerial glasses with the maximum concentrations increasing with water depth. The overwhelming dominance of degassed glasses on the submarine flanks of Mauna Loa implies that much of volcano's recent submarine growth involved subaerially erupted lava that reached great water depths (up to 3.1 km) via lava tubes. Anomalously high F and Cl in some submarine glasses and glass inclusions indicate contamination possibly by fumarolic deposits in ephemeral rift zone magma chambers. The relatively high CO_2 but variable H_2O/K_2O and S/K_2O in some submarine rift zone glasses indicates pre-eruptive mixing between degassed and undegassed magma within Mauna Loa's rift system. Volatile compositions for Mauna Loa magmas are similar to other active Hawaiian volcanoes in S and F, but are less Cl-rich than Lō'ihi glasses. However, Cl/K2O ratios are similar. Mauna Loa and Lō'ihi magmas have comparable, but lower H_2O than those from Kilauea. Thus, Kilauea's source may be more H_2O-rich. The dissimilar volatile distribution in glasses from active Hawaiian volcanoes is inconsistent with predictions for a simple, concentrically zoned plume model.

M.G. Davis · M.O. Garcia (✉)
Department of Geology and Geophysics,
University of Hawai'i, Honolulu, HI 96822, USA
E-mail: mogarcia@hawaii.edu

P. Wallace
Ocean Drilling Program, Texas A&M University,
College Station, TX 77845, USA

Present address: P. Wallace
Department of Geological Sciences,
University of Oregon, Eugene, OR 97403, USA

Editorial responsibility: E. Hauri

Introduction

Volatiles are important in volcanic systems because of their fundamental impact on the physical properties of host magma (e.g., temperature, density, and viscosity). They also provide revealing insights into magmatic crystallization, degassing, and contamination histories (e.g., Unni and Schilling 1978; Rowe and Schilling 1979; Gerlach and Graeber 1985; Garcia et al. 1989; Michael and Schilling 1989; Dixon and Stolper 1995; Hauri 2002). The release of volatiles from volcanic eruptions can also have dramatic atmospheric and climatic effects, and pose a significant hazard to both people and the environment (e.g., Rampino et al. 1988).

Active Hawaiian volcanoes are excellent natural laboratories for studying volatiles in basaltic magmas. Volcanic gases have been monitored at Kilauea Volcano since 1912 (e.g., Greenland 1987a) and at Mauna Loa since 1958 (Ryan 1995). These results and those from studies of volatiles in volcanic glasses (e.g., Garcia et al. 1989; Dixon et al. 1991; Gerlach 1993; Kent et al. 1999a; Dixon and Clague 2001) indicate that many processes may contribute to the volatile signature in Hawaiian magmas. Submarine glasses recovered from water depths >1 km generally have higher volatile contents compared with glasses from shallow submarine or subaerial eruptions because degassing is inhibited by the pressure of the overlying seawater (Moore 1965). However, some deep (>1 km) submarine-erupted lavas have highly variable H_2O and S concentrations, which have been attributed to mixing of low pressure degassed magma in the subaerial section of the rift zone with undegassed magma, followed by eruption on the submarine flanks (Dixon et al. 1991). Contamination adds a

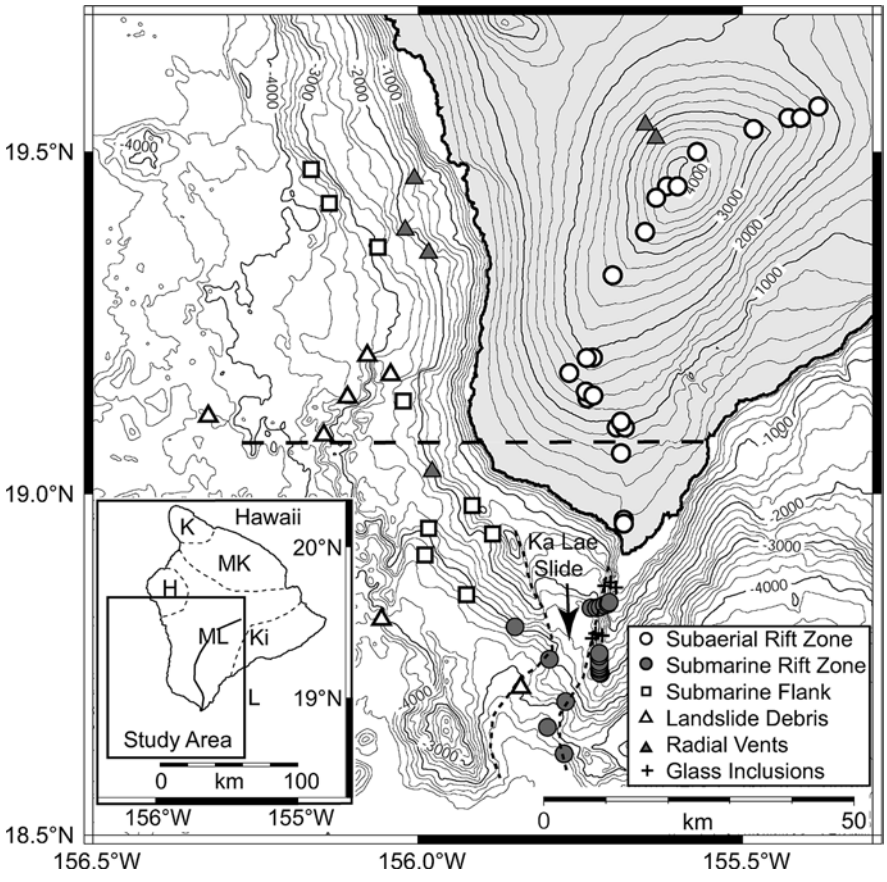

Fig. 1 Topographic map of the southwestern section of the island of Hawai'i showing where Mauna Loa samples were collected for this study. Only glass inclusions from samples collected along the submarine section of the southwest rift zone were analyzed. The *heavy dashed line* shows the location of the cross section in Fig. 9. The *inset map* gives the summit locations of the five subaerial volcanoes that comprise the island of Hawai'i (*K* Kohala, *MK* Mauna Kea, *H* Hualâlai, *ML* Mauna Loa, *Ki* Kilauea), the seamount Lō'ihi (*L*), and the study area. Mauna Loa's rift zones are designated by the *solid dark lines*. The western and eastern boundaries of the Ka Lae landslide are shown by the *short dashed lines*. The contour interval is 200 m

further complexity to understanding volatile data. Lō'ihi glasses commonly have elevated Cl contents, which have been interpreted to result from contamination by a seawater-derived component (Kent et al. 1999a, 1999b). These shallow level processes are superimposed on source heterogeneities within the Hawaiian plume (e.g., Byers et al. 1985; Garcia et al. 1989; Dixon and Clague 2001; Hauri 2002). Previous volatile studies have focused on submarine near-vent rift zone lavas giving an incomplete perspective on the processes controlling volatile abundances. To unravel the complex processes affecting volatiles in ocean island magmas, we undertook a comprehensive study utilizing near vent and distal subaerial and submarine lavas.

Mauna Loa is an ideal place to evaluate the "volatile story" for ocean island volcanoes. Fresh glass can be obtained from a wide variety of subaerial and submarine regions of the volcano (Fig. 1). In this paper we present major element and volatile compositions for quenched rinds from 114 submarine pillow basalts and 23 subaerial basalts and numerous olivine-hosted glass inclusions from mostly the southwest rift zone and western flank of Mauna Loa Volcano. This is the most extensive study of volatiles ever undertaken for a Hawaiian volcano. Below, we examine the effects of degassing and crustal contamination on volatile abundances in Mauna Loa glasses.

We use the results to evaluate the parental magma volatile contents for these glasses and compare them with those from two other active, tholeiitic Hawaiian volcanoes and comment on the implications of volatile distributions for the concentrically zoned plume model. Lastly, we propose a model for the growth of Hawaiian shield volcanoes.

Geologic setting

Mauna Loa, the Earth's largest volcano with a volume in excess of 80,000 km^3, is one of five volcanoes that compose the Big Island of Hawai'i (Fig. 1). It is an active shield volcano, with at least 39 historical eruptions between 1778 and 1984 (Barnard 1995). All but two of these eruptions were in its caldera or along its two rift zones. The exceptions are radial vent eruptions; one occurred in 1859 with vents at ~2,600 to 3,400 m above sea level (m a.s.l.) and the other in 1877 from vents between 120 and 1,000 m below sea level (m b.s.l.; Moore et al. 1985). The southwest rift is Mauna Loa's dominant rift zone. It is ~100 km long and has over 9 km of vertical relief.

The subaerial portion of Mauna Loa has been well characterized by numerous geologic and geophysical studies including mapping (e.g., Lockwood et al. 1988; Wolfe and Morris 1996), remote sensing (e.g., Kahle et al. 1995), gravity (e.g., Johnson 1995), seismicity (e.g., Okubo 1995), geochemistry (e.g., Rhodes 1988, 1995), and volcanic hazard potential (Trusdell 1995). Only

reconnaissance studies have been undertaken of the submarine portion of Mauna Loa including mapping (e.g., Moore and Chadwick 1995), seismic profiling (e.g., Hill and Zucca 1987), and petrology/geochemistry (e.g., Garcia et al. 1995b; Kurz et al. 1995). Submarine studies have focused on the southwest rift zone of Mauna Loa, the interior of which has been exposed by the Ka Lae landslide revealing a dike complex (Fornari et al. 1979b; Garcia et al. 1995b) that may be 15 km wide (Garcia and Davis 2001).

Samples

Most of the submarine glasses for this study are from 26 dredge hauls made on the western flank and southwest rift zone of Mauna Loa (Fig. 1) at water depths between 1,600 and 4,600 m b.s.l. during a 1999 R/V *Moana Wave* cruise (labeled with the prefer "M" followed by the dredge and sample numbers). The other submarine glasses and all of the olivine-hosted glass inclusions are from a 1991 submersible program (labeled by dive numbers 182–185; Garcia et al. 1995b) and a 1983 dredging cruise (samples with "ML" prefix; Garcia et al. 1989) along the southwest rift zone. Trace element and isotopic data are also available for many of these older sample sets (1991 samples, Garcia et al. 1995b; Kurz et al. 1995; 1983 samples, Gurriet 1988). This comprehensive suite includes samples from most morphologic regions of submarine Mauna Loa including the southwest rift zone, landslide debris, radial vents, and the western submarine flank (Fig. 1). Glassy-rimmed pillow lava is the dominant rock type collected from each submarine region except in the landslide areas. Seven dredge hauls in the landslide debris regions from the older South Kona landslide (Moore et al. 1995) and the younger Ka Lae landslide (Moore et al. 1989) recovered extremely diverse suites of lavas (20 or more distinct lithologies in each dredge haul including highly vesicular and oxidized lavas, sedimentary breccias and rare pillow lavas). Four new radial vents were discovered during our 1999 cruise at water depths of 1,200–2,000 m b.s.l. (Fig. 1). These vents have well-defined conical features with at least 100 m of relief and clearly post-date the several major landslides on the western flank of Mauna Loa. Dredge hauls on these vents recovered mostly monolithologic suites of pillow lavas with abundant fresh glass, some with Mn crusts containing the hydrothermal mineral todorokite (e.g., Hein et al. 1996), and abundant fauna. These features indicate that the cones are sites of recent eruptive activity.

The pillow rim lavas analyzed here are mostly weakly vesicular (average 2 vol%; range <1 to 30 vol%) with small round vesicles. Olivine is the dominant phenocryst (averaging 12 vol%, but ranging in abundance from <1 to 38 vol%) with no or minor amounts (<3 vol%) of plagioclase and clinopyroxene phenocrysts in a glassy matrix with or without plagioclase microlites. Olivine phenocrysts are generally euhedral, normally zoned, and contain abundant glass inclusions, which are round and mostly devoid of crystals (only rare spinel). Glass inclusions from 30 submarine rift lavas were analyzed for major elements, F, Cl, and S in this study. Care was taken to avoid inclusions that were intersected by cracks in the host olivine.

In addition, we analyzed glasses from 21 spatter and two lava rind samples from historic (after 1778) and prehistoric (up to ~30 ka, Lockwood et al. 1988) subaerial vents on Mauna Loa's summit area, and northeast and southwest rift zones. Vent elevations for these glasses range from 170 to 4,000 m a.s.l. In addition, two radial vent samples from the 1859 eruption at 3,350 and 2,600 m a.s.l. (Fig. 1) are included. The subaerial glasses are fresh, strongly vesicular with variable amounts of olivine phenocrysts and rare plagioclase microlites (<0.1 mm long).

Analytical methods

Glass compositions were measured using the University of Hawaii Cameca SX-50, five-spectrometer electron microprobe. Major element analyses were performed using a 15-kV accelerating voltage, 10-nA beam current, and a 10-μm diameter beam. Peak counting times were 60 s for Ti, Al, Fe, and P; 50 s for Si and Mg; and 40 s for Mn, Ca, Na, and K. Background counting times were half the peak time for each element. Natural glass and mineral standards were used for calibration. A PAP–ZAF matrix correction was applied to all analyses. Two-sigma precision based on counting statistics is $<1\%$ for major elements, and $<5\%$ for minor elements (K, Mn, P). Reported analyses are the average of five spot analyses for the pillow rim glasses and three to five spots for the glass inclusions.

Experimental procedures were developed following the procedures of Robinson and Graham (1982) and Thordarson et al. (1996) for microprobe analysis of F, Cl, and S to minimize both the uncertainty and the minimum detection limit of the analyses without degassing the volatiles or making the analysis time unnecessarily long. These analyses were carried out after the major element analyses and on a different spot using an 80-nA beam current. The spectrometer crystals, PET for S and Cl, and PC0 for F, were optimized for maximum intensities. Peak and background counting times were 400 and 200 s, respectively. In addition to using a 10-μm defocused beam, the beam was "blanked" using the faraday cup every 20 s for a period of 4 s during peak counting times to minimize volatilization and oxidation of the glass and standard. This is important for S because oxidation will change its peak location and lower count rates (Wallace and Carmichael 1994). The calibration standards were troilite (S), scapolite (Cl), and fluorophlogopite (F). Troilite was selected after determining that reduced S (S^{-2}) is the dominant species in Mauna Loa glasses using the procedures of Wallace and Carmichael (1994). Similar results were reported for Hawaiian and other submarine tholeiitic basalt glasses (e.g., Byers et al. 1985; Wallace and Carmichael 1994). Fluorophlogopite was used because it showed no volatilization during analysis at beam currents of 80 nA, unlike apatite, which lost significant F after ~100 s (at least 30%) despite efforts to minimize sample devolatilization. The major element content of each glass was used to apply the appropriate PAP–ZAF matrix correction. This post-analysis matrix correction increased S by ~10% and decreased Cl and F by ~10%. We also found an average ~5% difference between volatile abundances using the compositionally similar glass standard VG-2 (Jarosewich et al. 1979) versus the actual major element composition of the glass.

Two-sigma precision for these analyses based on counting statistics is ±26 ppm (~2%) for S, ±25 ppm (5–8%) for Cl, and ±30–40 ppm (6–12%) for F. Reproducibility (2σ) of the glass sample standard VG-2 (Jarosewich et al. 1979), TR138-6D-1,

Table 1 Analyses of total H_2O, molecular H_2O, and carbonate in selected submarine glasses from Mauna Loa. All data are determined by FTIR using procedures described in the text. Data for total H_2O and molecular H_2O are in wt%; data for carbonate are expressed as the equivalent amount of CO_2 in ppm. *b.d.* Below detection

Sample	Total H_2O	±2 SD	H_2O_{mol}	CO_2	±2 SD
Submarine rift zone					
182-3	0.17	0.01	b.d.	25	4
183-3	0.27	0.02	b.d.	b.d.	–
184-2	0.37	0.02	0.02	40	5
184-8	0.39	0.03	0.02	26	4
184-9	0.20	0.02	b.d.	b.d.	–
184-11	0.10[a]	0.01	b.d.	[b]	–
185-1	0.45	0.07	[b]	[b]	–
185-2	0.33	0.02	0.02	79	11
185-3	0.30	0.03	b.d.	86	13
185-10	0.24	0.02	b.d.	81	12
M1-02	0.25	0.01	b.d.	166	20
M2-03	0.73[c] (0.67)	0.03	0.13	154	19
M2-05	0.39	0.08	[b]	[b]	–
M3-02	0.87[c] (0.73)	0.09	0.22	[b]	–
M4-03	0.20	0.01	b.d.	212	26
M4-11	0.46	0.03	0.04	214	28
Other submarine areas					
M6-19	0.11[b]	0.01	b.d.	b.d.	–
M14-08	0.11[b]	0.01	b.d.	b.d.	–
M15-52	0.09[b]	0.01	b.d.	b.d.	–
M24-H	0.09	0.01	b.d.	b.d.	–
M30-01	0.47	0.03	0.03	132	18

[a]Minimum value for total H_2O because the glass was so filled with microlites that no microlite-free region of glass could be analyzed
[b]Absorption bands for H_2O_{mol} and carbonate were obscured by absorption bands from abundant microlites in the glass
[c]Glass contains excess molecular H_2O, probably due to low temperature hydration. Values in parentheses are "corrected" magmatic values calculated by subtracting the excess molecular H_2O

TR138-7D-1, and TR154-21D-3 (Michael and Schilling 1989), over a period of several months was ±20 ppm (~1%) for S, ±15 ppm (~5%) for Cl, and ±50 ppm (9–17%) for F. Our precision is comparable to those using higher currents and longer count times. Our minimum detection limits are 30 ppm for both S and Cl and 80 ppm for F. K_2O and FeO were also measured along with the volatiles to improve the precision of these oxides and to provide an online correction for the interference of Fe with F (Todd 1996). Without this correction, measured values of F are about three times greater than actual. The 2σ precision improved to ~2.5% for K_2O and ~0.65% for FeO using the longer counting times. Reported volatile analyses are the average of two to five spots.

Glass inclusions from three of the samples (182-8, 183-15, and 184-7, labeled "h") were homogenized by heating the host olivine to temperatures based on their composition and phase equilibria experiments on Mauna Loa lavas (Montierth et al. 1995) for about an hour. The olivine core compositions are nearly homogeneous with values of forsterite 86 to 89. Heating temperatures for the olivines were 1,240 to 1,270 °C, respectively. The oxygen fugacity in the furnace was controlled at the FMQ buffer.

Total H_2O, molecular H_2O, and CO_2 (present as carbonate, CO_3^{2-}) were measured for 21 glass samples using Fourier transform infrared (FTIR) spectroscopy. The quantitative procedures, band assignments, and calibrations used are from Dixon et al. (1995) and Dixon and Pan (1995); a complete description of these procedures is given in Wallace (2002). Dissolved carbonate was measured from the absorbances of the bands at 1,515 and 1,430 cm^{-1} (Fine and Stolper 1986; Dixon et al. 1995). Because the shape of the background in the region of the carbonate doublet is complex, absorbance intensities for the 1,515- and 1,430-cm^{-1} bands were measured after subtraction of a reference spectrum for a decarbonated Kilauea basaltic glass to achieve a relatively flat background (Dixon et al. 1995). The molar absorptivity for carbon dissolved as carbonate in basaltic glasses is compositionally dependent (Dixon and Pan 1995). Dissolved carbonate contents (reported in Table 1 and hereafter as the equivalent amount of CO_2, in ppm) were determined using a molar absorption coefficient of 353 ± 71 mol^{-1} cm^{-1}, calculated from the average composition of the glasses and the linear equation reported by Dixon and Pan (1995).

The analysis of some glass samples was complicated by the presence of abundant microlites. The total H_2O concentrations reported for four of the most microlite-rich glasses represent minimum values because no totally glassy area could be found for analysis. However, these four samples all have very low total H_2O (~0.1 wt%), and visual estimates of the proportion of microlites suggests that the true glass H_2O concentrations are no more than ~30% greater than the reported value. Abundant microlites also caused a problem in analyzing carbonate in some glasses because of an Si-O peak at ~1,550 cm^{-1} that partially to totally obscures one of the peaks (1,515 cm^{-1}) in the carbonate doublet. In some cases it was possible to correct for this by using a degassed, microlite-bearing glass for the reference background subtraction, but in four glasses the problem of microlites prevented us from determining the carbonate concentration.

Precision ($\pm 2\sigma$) of the total H_2O measurements is generally <10%, but is greater for several samples for which very thin (<50 μm) wafers of glass were analyzed. Precision for the molecular H_2O analyses is ±0.01 to 0.02 wt%, and for the carbonate analyses, about ±15%. Accuracy with these techniques is estimated to be ±10% for total H_2O, and ±20% for CO_2 and molecular H_2O (Dixon and Clague 2001).

Major elements

The submarine and subaerial glasses, and olivine-hosted glass inclusions examined here are tholeiitic in composition and have similar major elements abundances as other published for Mauna Loa glass analyses (Fig. 2; Appendix 1). However, the range of MgO concentrations for the matrix glasses extend to more evolved compositions than noted in previous studies (4.5–8.0 vs. 5.5–8.2 wt%). Most of the evolved samples (<7 wt%) are from the volcano's submarine flank. The new MgO glass contents indicate quenching temperatures of 1,115–1,196 °C based on the Montierth et al. (1995) Mauna Loa empirical glass geothermometer. The glass compositions define curved or kinked trends on MgO variations diagrams as predicted by MELTS crystal fractionation modeling (Fig. 2). Thus, crystal fractionation has played an important role in controlling compositional variation of these Mauna Loa lavas. The breadth of the compositional variation at a given MgO value reflects a wide range in parental magma composition.

The glass inclusions also have a broad MgO range that extends to higher and lower values than the glasses (2.6 to 11.4 wt%), although many of the inclusions are comparable with the glasses (Fig. 2). Most of the evolved glass inclusions have much higher CaO and lower K_2O than the matrix glasses and some inclusions have distinctly lower Al_2O_3 (Fig. 2). Some of the high MgO inclusions have low FeO contents, which is indicative of post-entrapment crystallization and diffusion (Danyushevsky et al. 2000; Gaetani and Watson 2000). Multiple glass inclusions were analyzed for some

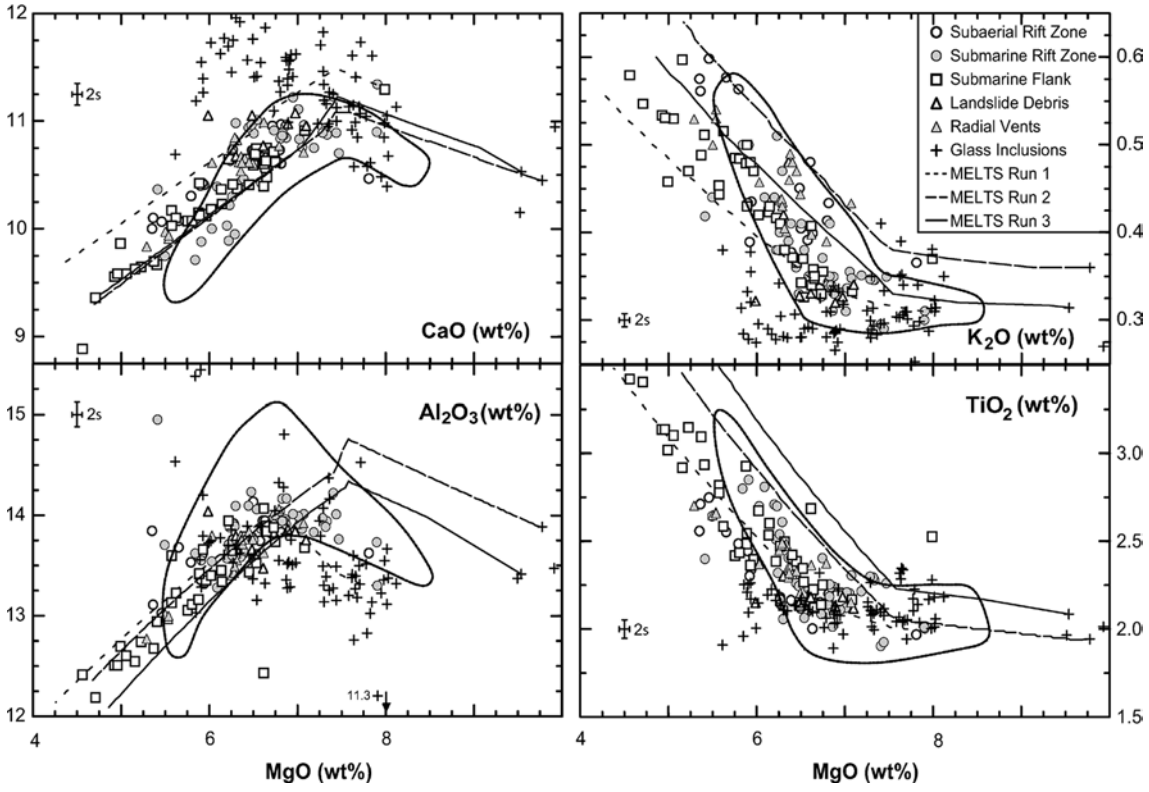

Fig. 2 MgO variation diagrams for select major element oxides. Most of the pillow rim glass data fall within the fields for published Mauna Loa glasses (data from Garcia et al. 1989, 1995b; Moore and Clague 1992; Moore et al. 1995; Garcia 1996). The glass inclusion data show greater compositional diversity than the pillow rim glasses. Liquid lines of descent for three crystal fractionation models (MELTS; Ghiorso and Sack 1995) are also shown for three possible parent compositions for Mauna Loa lavas (see text for modeling details). Two sigma error bars are given for reference

samples and large compositional variations were found. Some of this variation reflects different degrees of post-entrapment crystallization, but, even at the same degree of fractionation, significant compositional variation is present (e.g., 0.25–0.39 K_2O at 7.7 wt% MgO). This compositional variation cannot be explained by crystal fractionation or magma mixing involving any basaltic minerals or observed magma compositions. Similar results have been reported for other Hawaiian lavas (Clague et al. 1995) and were explained by pooling of melts from a heterogeneous source after formation of olivine crystals (e.g., Sobolev et al. 2000). See Appendices 1 and 2 for complete copy of glass and glass inclusion dataset.

Volatiles

Sulfur

Mauna Loa glasses range widely in volatile content (Fig. 3). For example, S contents vary from 68–373 ppm for subaerial glasses and from 32–1,422 ppm for submarine ones (Appendix 1). The submarine values are 40% higher than previous reported for Mauna Loa glasses, but are within the range reported for submarine tholeiitic glasses from other Hawaiian volcanoes (e.g., Garcia et al. 1989). Olivine-hosted glass inclusions have a similar S range as the submarine glasses (65–1,568 ppm; Appendix 2), but are more variable than those previously reported (341–777 ppm; Hauri 2002). The highest S concentrations are near or somewhat above the mid-ocean ridge basalt (MORB) S-saturation line (Fig. 4). High S contents also are observed in Lō'ihi glasses and are thought to be caused by their generally higher f_{O2} relative to MORB, which results in higher S for basaltic melts in equilibrium with immiscible sulfide liquid (Wallace and Carmichael 1992). An examination of thin sections for the Mauna Loa high S glasses revealed that sulfide blebs are absent or extremely rare in contrast to Lō'ihi glasses (Yi et al. 2000). This indicates Mauna Loa magmas are probably more oxidized than MORB and many Lō'ihi magmas. There is a weak correlation of S with FeO for glasses with lower S concentrations (<200 ppm; Fig. 4). All but one of the Mauna Loa subaerial samples have S concentrations less than 220 ppm, which is typical of Kilauea subaerial lavas and attributed to S degassing (e.g., Moore and Fabbi 1971; Swanson and Fabbi 1973). Most of the submarine flank glasses (non-rift) also have low S concentrations, similar to the subaerially erupted glasses (Fig. 3), with the lowest S abundances found in the landslide debris glasses (32–105 ppm). Similar results were reported for glasses collected in deep water ($>4{,}000$ m b.s.l.) from South Kona landslide (Moore et al. 1995).

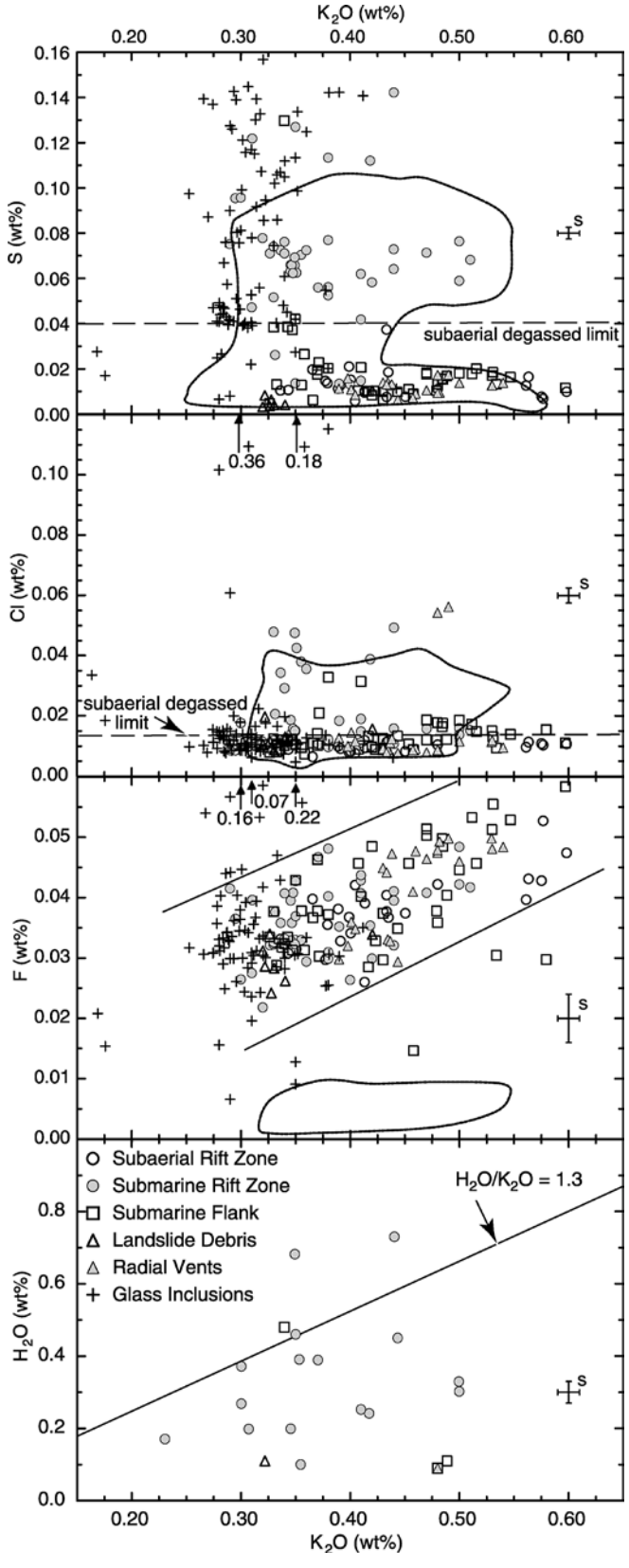

Most submarine rift zone samples have higher S than other submarine glasses and there is an overall increase in maximum S content with the water depth

Fig. 3 Plots of S, Cl, F, and H_2O versus K_2O for Mauna Loa glasses. Contents of S, Cl, and H_2O do not correlate with K_2O, indicating that degassing or some other process has affected the abundances of these volatiles. The field shows previous data for Mauna Loa glasses (from Garcia et al. 1989, 1995b; Moore and Clague 1992). The Kilauea H_2O/K_2O reference line of Wallace and Anderson (1998) is given for comparison. The two Mauna Loa samples with anomalously high H_2O/K_2O have probably been affected by assimilation involving brine, causing elevated H_2O and Cl (see Fig. 10). In contrast to S, Cl, and H_2O, F contents broadly correlate positively with K_2O, indicating that F degassing is minor for Mauna Loa eruptions. In the F and Cl plots, an *arrow* and a value are given for glass inclusion data that plot off the diagram. Two-sigma error bars are given for reference

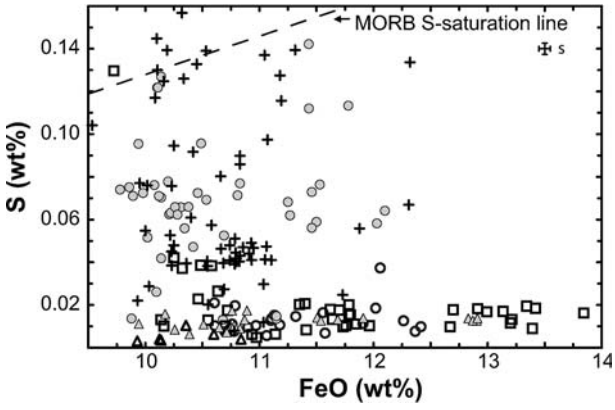

Fig. 4 Total iron as FeO versus S plot for Mauna Loa glasses. The highest pillow rim glass S values are near the MORB S-saturation line (*dashed line*) of Mathez (1976). Most submarine rift samples (glasses and glass inclusions) have S abundances > 400 ppm; all but one of the subaerial and non-rift submarine glasses have lower S concentrations (< 300 ppm). Two sigma error bars are given in the *upper right corner* of the plot. *Symbols* are on Fig. 2

for rift glasses to 3,700 m b.s.l. (Fig. 5). This is consistent with the general observation that S degassing occurs in lavas erupted subaerially or in shallow submarine conditions (e.g., Moore and Fabbi 1971). However, as noted in previous studies (Garcia et al. 1989; Moore and Clague 1992; Garcia et al. 1995b), there is considerable scatter in S content with water depth for Mauna Loa submarine rift glasses (Fig. 5). These results indicate that lavas erupted in deep water have partially degassed S at some point during their magmatic history (Fig. 5).

Chlorine

The Cl abundances for our Mauna Loa glasses range from 64–119 ppm for subaerial samples and 70–560 ppm for submarine ones (Fig. 3; Appendix 1). A study of subaerially-erupted Kilauea glasses found Cl concentrations of 51–106 ppm (Swanson and Fabbi 1973), nearly identical to the range observed here for Mauna Loa subaerial glasses. The highest Cl value (560 ppm) is 50% greater than previously reported for Mauna Loa submarine glasses, but well within the range reported for

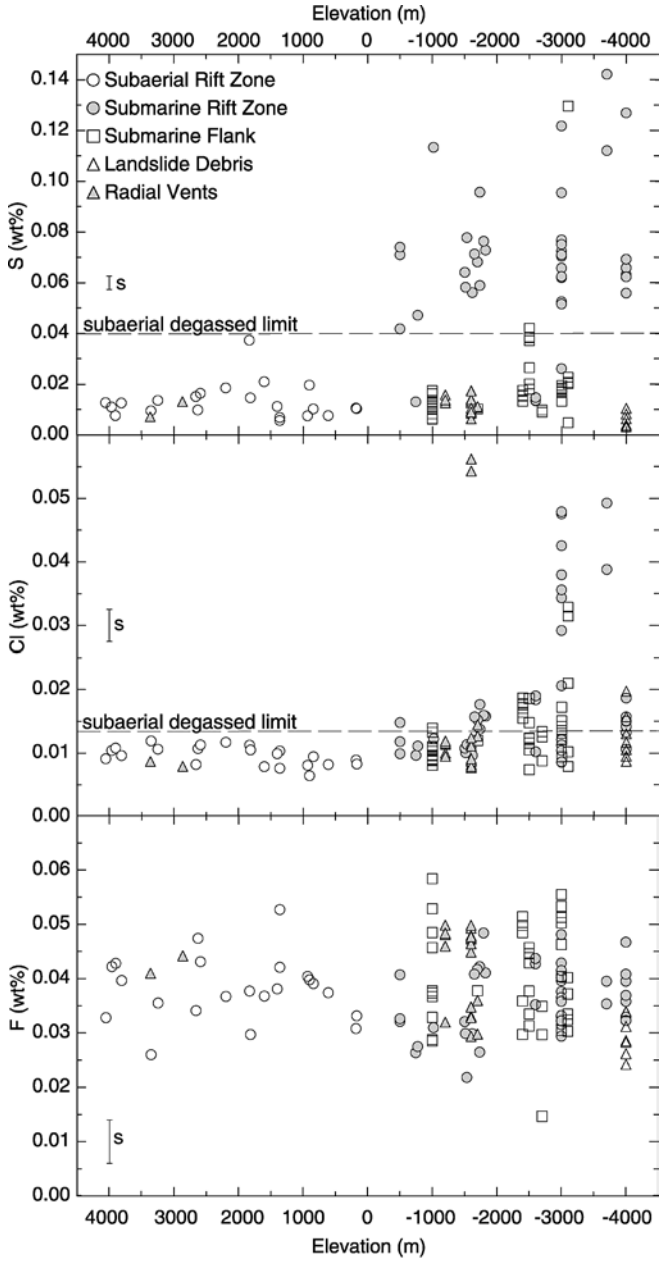

Fig. 5 Plots of S, Cl, and F abundances versus elevation for Mauna Loa glasses. The maximum content of S increases with eruption depth below sea level only (with one exception) for rift zone erupted glasses. All but one of the non-rift submarine glasses have low S (< 450 ppm), even for lavas recovered at depths > 1 km. Cl increases with eruption depth below sea level with a major increase at 3 km. Two glasses from one of the radial vents have the highest Cl, but contain low S abundances. Contents of F do not correlate with elevation. Submarine elevations for dredged rocks (see Appendix 1) are minimum depths. Two-sigma error bars are given for reference

Hawaiian tholeiitic glasses (e.g., Kent et al. 1999a). Glass inclusion Cl abundances range from 47–3,653 ppm (Appendix 2), which are greater than those previously reported for Mauna Loa (58–95 ppm; Hauri 2002) and include the second highest concentration ever reported for a Hawaiian glass (highest value is 11,053 ppm for a Lō'ihi glass inclusion; Hauri 2002). However, the majority of submarine glasses and glass inclusions have < 200 ppm Cl. There is a slight correlation of Cl with water depth, particularly along the rift zone if glasses with > 300 ppm Cl are excluded (Fig. 5; high Cl glasses will be discussed below). The decrease in Cl with decreasing depth of collection along the rift is indicative of Cl degassing, which was noted in a study of Icelandic submarine basalts erupted at a shallower water depths (< 500 m b.s.l., Unni and Schilling 1978; vs. < 2,000 m b.s.l.; Fig. 5). Two submarine glasses from the southernmost radial vent (M24; Fig. 1) have the highest Cl abundance (~550 ppm), which is about five times greater than other radial vent and subaerial glasses, but they have low S contents (~175 ppm).

Fluorine

Mauna Loa subaerial glasses range in F contents from 260 to 527 ppm; submarine glasses range from 147 to 580 ppm (Appendix 1). Glass inclusions have a much wider range of F contents (90–2,240 ppm; Appendix 2). These F abundances are much greater (~2.5 times) than previously reported for Mauna Loa submarine glasses (Garcia et al. 1989), but are comparable to some new glass inclusion data (336–969 ppm; Hauri 2002). The previous data may be anomalously low due to absorption of F by the heating vessel (D. Muenow 2001, personal communication). The new data are similar to values reported for submarine Lō'ihi and subaerial Kilauea tholeiitic glasses (Swanson and Fabbi 1973; Byers et al. 1985). There is a broad correlation between F and K_2O (Fig. 3) and other incompatible oxides (P_2O_5 and TiO_2), but no apparent correlation of F with elevation (Fig. 5). These results are similar to those for glasses from Iceland and the Reykjanes Ridge, which have been interpreted to indicate that F degassing is minor during subaerial eruptions (Rowe and Schilling 1979; Sigvaldason and Oskarsson 1986). However, a study of lavas from the Laki eruption suggested extensive F degassing (up to 50%; Thordarson et al. 1996). This issue will be discussed below.

Water

Concentrations of H_2O in Mauna Loa submarine glasses range widely (0.09–0.87 wt%; Table 1; Fig. 3). The ratios of molecular H_2O to total H_2O for most glasses are close to the high temperature equilibrium speciation curve for basaltic melts (Dixon et al. 1995). However, the two glass samples with the highest total H_2O (M2-3 and M3-2) show an excess of molecular H_2O relative to the speciation curve, suggesting these samples have been affected by low temperature alteration. It is possible to estimate the original magmatic H_2O concentration for these two glasses by subtracting the excess molecular

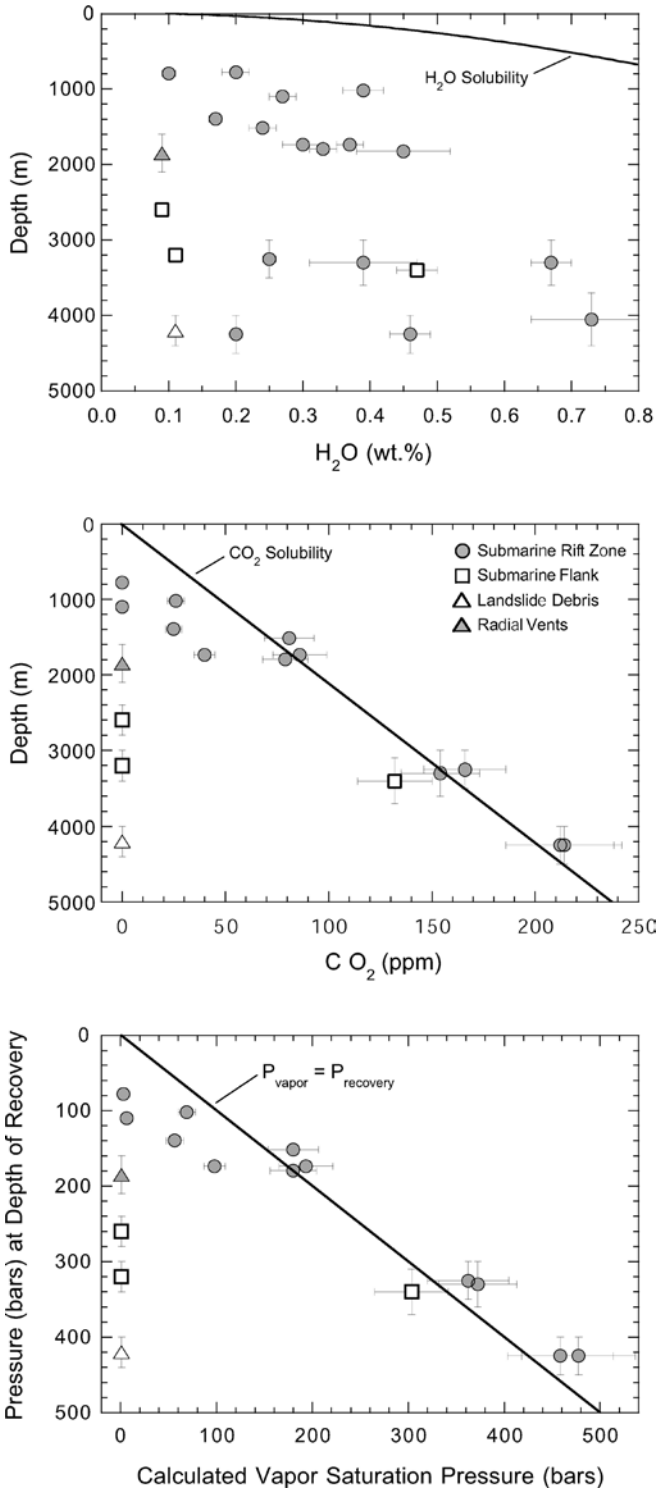

Fig. 6 Plots of **a** H_2O and **b** CO_2 versus recovery depth, and **c** inferred vapor saturation pressure vs. pressure of recovery for Mauna Loa submarine glasses. H_2O contents show no relationship to recovery depth. Five of the glasses, recovered from $<1{,}000$ to $>4{,}000$ m, have $\sim$0.1 wt% H_2O, similar to the 1 bar solubility value for basaltic melt. The same glasses have essentially no CO_2. In contrast, CO_2 in submarine rift zone glasses (and one submarine flank glass) show excellent correlation with recovery depth, indicating that they were saturated with CO_2-rich vapor at the time of eruption. However, several submarine rift glasses are slightly offset from the solubility curve, suggesting they flowed to greater water depth during eruption. Solubility curves for H_2O and CO_2 in basaltic melts are calculated from Dixon et al. (1995) assuming hydrostatic pressure. Vapor saturation pressures for individual glasses shown in **c** are also calculated using Dixon et al. (1995). Two sigma error bars for H_2O and CO_2 are given for reference; where no error bar is shown, the uncertainty is smaller than the *symbol*. *Vertical error bars* show uncertainties in depth of recovery for dredged samples

water (Table 1). Although the uncertainty associated with this procedure is difficult to assess, the magnitude of the correction is small (0.06 to 0.14 wt% H_2O), and after correction, these two samples still have relatively high total H_2O ($\sim$0.7 wt%). These samples also have elevated concentrations of Cl (Appendix 1).

Total H_2O contents show no correlation with water depth of recovery, and all glasses are H_2O-undersaturated for their collection depth relative to the solubility curve for basaltic melts (Fig. 6). The most water-poor glasses (five samples with $\sim$0.1 wt%) have H_2O concentrations that are typical of values obtained for subaerially erupted Hawaiian tholeiitic lavas (Swanson and Fabbi 1973). These low concentrations correspond to the 1 bar solubility value for H_2O in basaltic melts (Dixon et al. 1995). H_2O values for the other glasses are similar or somewhat higher than those found in a previous study of Mauna Loa submarine rift glasses (0.18–0.55 wt%; Garcia et al. 1989). There is no correlation between H_2O and Cl (Fig. 7), or H_2O and K_2O (Fig. 3), despite the good correlation of K_2O with other incompatible elements such as P_2O_5. However, H_2O is well correlated with S (Fig. 7). Seventy-five percent of the glasses have $H_2O/K_2O < 1.3$ (Fig. 3), the value that is thought to be representative of Kilauea parental tholeiitic magmas (Wallace and Anderson 1998). Very low H_2O/K_2O ratios (0.5) are indicative of H_2O degassing. However, intermediate H_2O/K_2O values ($\sim$0.9) were observed in Lō'ihi submarine glasses and were attributed to a mantle source that is depleted in H_2O (Dixon and Clague 2001).

Carbon dioxide

Abundances of carbon dioxide in Mauna Loa glasses vary from below the detection limit (<20 ppm CO_2) to 214 ppm (Table 1). About half of the FTIR-analyzed glasses have CO_2 concentrations that are close to the CO_2 solubility curve for basaltic melts at the pressure of recovery (Fig. 6). The other samples, including six with CO_2 abundances below our detection limit, are CO_2 undersaturated. A subset of undersaturated glasses (182-3, 183-3, 184-2, -8, -9, and M30-01; all but the last sample were collected in place by a submersible) have CO_2 contents that suggest they were recovered about 500–1,000 m deeper than would be predicted if they were saturated with CO_2-rich vapor at the time of eruption

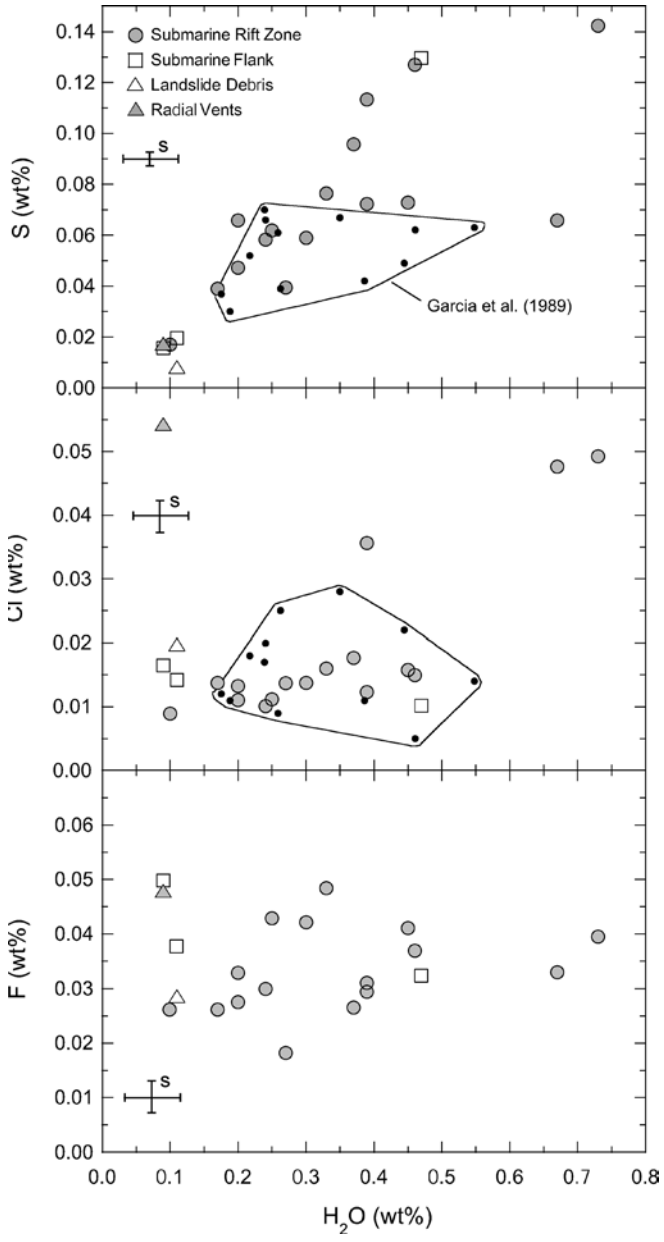

Fig. 7 S, Cl, and F versus H_2O plots for Mauna Loa glasses. *Small filled circles* show Mauna Loa data from Garcia et al. (1989). F data from this earlier study were not plotted because values are anomalously low due to absorbance by the heating vessel. S contents generally correlate with H_2O, indicating that the abundances of these volatiles are affected by degassing. The samples that plot off this trend have excess molecular water (see Table 1). Cl contents do not correlate with H_2O indicating some other process such as crustal assimilation is responsible (see text for discussion). Two sigma error bars are given for reference

(Fig. 6). The low CO_2 contents could result from downslope flow of the sample during eruption and/or the gradual subsidence of Mauna Loa Volcano. The four glasses that are strongly CO_2 undersaturated (M6-19, M14-08, M15-52, M24-H) all have very low H_2O (~0.1 wt%). The cause of low CO_2 and H_2O in these deep water glasses is discussed in the next section.

Volatile degassing at Mauna Loa Volcano

Volatile degassing is a critical driving force for volcanic eruptions (Jaggar 1940). The solubility of magmatic volatiles is controlled primarily by pressure, so the extent of degassing during an eruption depends on ambient pressure. The solubility of CO_2 in basaltic melts is very low, and as a result, most of the primary CO_2 in Hawaiian basaltic magmas is degassed during crustal storage (Gerlach and Graeber 1985; Dixon and Clague 2001). In contrast, S, Cl, F, and H_2O, which are much more soluble than CO_2, remain dissolved in basaltic magmas during crustal residence except during eruption. However, if the eruption occurs underwater, magmatic S, Cl, F, and H_2O concentrations may be quenched into the pillow rim glasses if the water depth is sufficiently deep. Although this depth will vary with absolute volatile concentration (primarily H_2O) and is influenced by several other magmatic factors, critical minimum water depths have been recognized for some ocean island volcanic systems. For Iceland, the critical depth for the start of S, H_2O, and Cl degassing was found to be ~500 m b.s.l. (Unni and Schilling 1978). For Hawai'i, the critical depth for H_2O and S degassing is thought to be ~1,000 m (e.g., Moore 1970; Moore and Fabbi 1971). Insufficient Cl data were available to assess its critical degassing depth in Hawai'i . F degassing has not been evaluated for Hawaii and is controversial for Iceland. The notion of a critical degassing water depth is complicated by the observation that some Kilauea lavas drain back into the volcano's magmatic plumbing system after eruption (e.g., Jaggar 1947; Richter et al. 1970; Wallace and Anderson 1998), mix with undegassed magma, and erupt later as partially degassed magma under even deep submarine conditions (e.g., Dixon et al. 1991).

Mauna Loa would seem to be an excellent volcano to evaluate degassing processes. It has a well-defined magmatic plumbing system, including a summit magma chamber that rises to ~1 km above sea level (Decker et al. 1983), and its vent system has over 9 km of relief. We systematically sampled this vent system to evaluate the effects of ambient pressure on magma degassing. Degassing of Cl and S is obvious for our suite of subaerial Mauna Loa glasses (Fig. 5). All of the subaerial glasses have low Cl contents (<0.014 wt%) and all but one of the glasses have low S concentrations (<0.022 wt%). Shallow submarine samples (<1 km water depth) show considerable scatter in S concentrations with values similar to and higher than the subaerial glasses (Fig. 5). The same pattern is evident for samples collected in deeper water (>1 km).

The vast majority of glasses collected away from the submarine rift zone have low S and Cl concentrations, despite being recovered from water depths $>1{,}000$ m b.s.l. It is possible that some of the dredged pillow lavas were transported from shallower water. However, a study of a submersible-collected suite of

in-place pillow lava glasses from the same flank of Mauna Loa found that 24 of 25 glasses have low S (< 300 ppm; Garcia and Davis 2001). An additional factor that might explain some of the scatter in volatile data is Mauna Loa's ~2.5 mm/year subsidence (Moore et al. 1990), which has been estimated to have caused ~400 m of subsidence of the submarine southwest rift zone (Garcia et al. 1995b). Nonetheless, the low S and Cl contents of the flank glasses are indicative that the vast majority of the pillow lavas on the deeper flanks (> 1 km) of Mauna Loa are degassed.

Glasses taken along Mauna Loa's southwest rift zone fall into three groups based on their S contents (Fig. 5). The first is the subaerially degassed glasses (S < 400 ppm); the second group is undegassed submarine glasses with S abundances near the MORB S-saturation trend (> 800 ppm; Fig. 4). The last group is submarine glasses with intermediate S concentrations (Fig. 4). These three S groups show a positive correlation with H_2O/K_2O (Fig. 8). H_2O/K_2O values below 0.5 probably have subaerially degassed, based on their low S (< 200 ppm). The two glasses with H_2O/K_2O of 1.6 and 1.9 and have elevated Cl, perhaps due to contamination (see below). The high S glasses have H_2O/K_2O of 1.0–1.4 indicating they are undegassed. However, these glasses contain variable CO_2 contents (26–214 ppm), perhaps from erupting CO_2-rich vapor-saturated magmas at variable water depths. The glasses with intermediate S contents have intermediate H_2O/K_2O (0.57–0.90) suggesting partial loss of H_2O and S by degassing. However, some of these glasses also have high CO_2 contents (up to 212 ppm) suggesting vapor saturation at the time of eruption. Drainback of degassed lava into underground reservoirs has been witnessed at many Kilauea eruptions (e.g., Jaggar 1947; Richter et al. 1970). The mixing of this degassed lava with undegassed magma was proposed to explain the hybrid volatile signature (low H_2O/K_2O and S, but high CO_2) in glasses from Kilauea's east rift zone of (Dixon et al. 1991). The same process may be occurring at Mauna Loa indicating that mixing of degassed and undegassed magmas may be a common process in ocean island volcanoes.

Fig. 8 Plots of S versus the ratios of Cl/K_2O, F/K_2O, and H_2O/K_2O for Mauna Loa glasses. The positive correlation between H_2O/K_2O and S indicates that H_2O and S are coupled in the degassing process. In contrast, there is no correlation of Cl/K_2O or F/K_2O with S indicating that the high ratios for the halogens are not the result of low pressure degassing. Instead, high Cl/K_2O, F/K_2O ratios are likely the result of contamination by hydrothermal deposits or a seawater-influenced component. The few samples with low F/K_2O values have low S abundance indicating possible F degassing. Two sigma error bars are given for reference

Implications of degassed pillow lavas for the submarine growth of Mauna Loa Volcano

Two contrasting models have been proposed for the structure of Hawaiian volcanoes. An early model suggested that these volcanoes contain a 0.2–2-km-thick wedge of fragmental debris, which mantles a ≥5-km-thick pile of pillow lavas (e.g., Moore and Fiske 1969; Fornari et al. 1979a). More recently, side-scan sonar images and observations of historical eruptions of Kilauea led Moore and Chadwick (1995) to propose that fragmental debris, mostly hyaloclastite produced by the shattering of lava as it enters the ocean, is the dominant lithology within ocean island volcanoes (> 7 km thick on the western flank of Mauna Loa; Fig. 9A). In this model, pillow lavas are a minor component of the volcano and

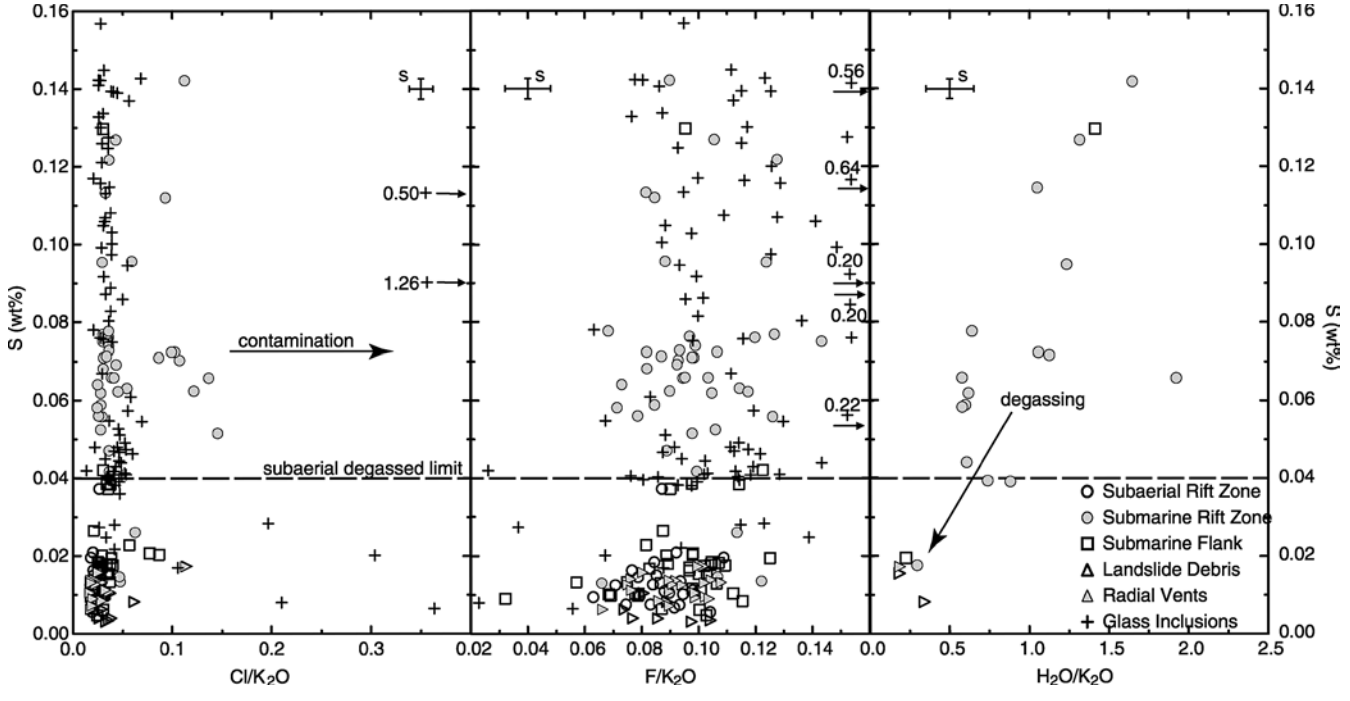

are formed primarily during the submarine phase of growth. However, this model conflicts with submersible observations at water depths up to 2 km and distances of ~10 km from the coast of Mauna Loa Volcano, which reported that pillow lavas are abundant and that fragmental debris are rare (Fornari et al. 1979a, 1980; Garcia and Davis 2001). Resolving whether Hawaiian volcanoes are comprised of predominantly fragmental debris will have a major impact on the landslide hazard potential of oceanic island volcanoes, on seismic velocity models for these volcanoes, and our understanding of the submarine growth of ocean island volcanoes.

Our new investigation indicates that degassed pillow lavas extend to great depths and distances from the coast (to at least 3,100 m b.s.l. and 20 km), and cover major portions of the western flank of Mauna Loa (Fig. 1). These results confirm the model of Garcia and Davis (2001) that subaerially erupted pillow lavas are the dominant rock type on the flanks of this Hawaiian volcano (Fig. 9B). These lavas probably crossed the shoreline in lava tubes or in lava streams under an insulating crust, which have been observed at both Kilauea and Mauna Loa Volcanoes (Tribble 1991; Garcia and Davis 2001). The pillow lava model also implies that oceanic island volcanoes have a more stable foundation than previously suspected, despite numerous landslides (e.g., Moore et al. 1989, 1994). Perhaps these landslides are more common shortly after a volcano's emergence above sea level, when fragmental material is overlain by subaerial flows. This model is analogous to the current eruption of Kilauea, where hyaloclastite is overlain by subaerial flows creating coastal benches that periodically collapse (Tribble 1991).

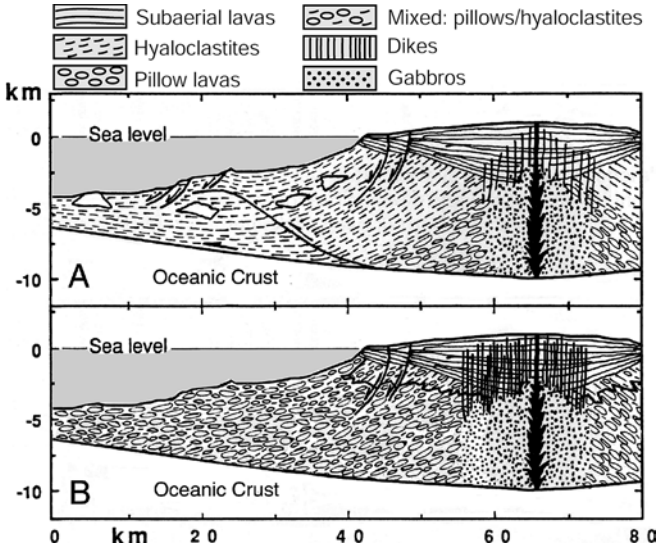

Fig. 9 Geologic cross section cartoons of the southwest rift zone of Mauna Loa (see Fig. 1 for location) showing the hyaloclastite (**A**; Moore and Chadwick 1995) and the pillow lava models (**B**; Garcia and Davis 2001). Our results show that degassed pillow lavas are the dominant rock type on the submarine flanks of Mauna Loa Volcano. Vertical exaggeration is two times (after Garcia and Davis 2001)

The glasses from seven dredge hauls made in areas of hummocky terrain, 15–45 km west of the current shoreline and at depths >2,500 m b.s.l. (Fig. 1) are a special case. These glasses all have very low S and Cl concentrations (Fig. 5). We interpret the low volatile content and high vesicularity of these glasses, the oxidized appearance of many rock samples, and the hummocky terrain where these samples were collected to indicate that these rocks were transported from subaerial Mauna Loa to deep ocean depths by landslides. Moore et al. (1995) reached the same conclusion for other Mauna Loa deep submarine samples. The several major landslides along the flanks of Mauna Loa have contributed significant quantities of subaerially erupted lavas to the ocean floor around the base of the volcano including blocks up to 12 km long.

F degassing?

Fluorine is by far the most soluble volatile in magmas at low pressures (e.g., Carroll and Webster 1994; Lange 1994). Nonetheless, a controversy exists concerning the extent of F degassing in basaltic magmas. Data for glasses from Iceland and the Reykjanes Ridge were interpreted to show little evidence of F degassing (Rowe and Schilling 1979; Sigvaldason and Oskarsson 1986). In contrast, a study of volatiles in glasses from the Laki 1783–1784 eruption in Iceland argued for up to ~50% F degassing during the eruption, with half of this loss at the vents and the rest during lava transport and cooling (Thordarson et al. 1996). This interpretation was based on comparing volatile abundances in glass inclusions with matrix glasses. F degassing during the Laki eruption was attributed to fluxing by effervescing volatiles (CO_2, H_2O, and S; Thordarson et al. 1996). However, an earlier Iceland study argued that fluxing is an ineffective method for removing F (Rowe and Schilling 1979). There is ample evidence from Iceland of F gas from eruptions killing livestock and being absorbed onto ash particles (Oskarsson 1980), but it has been argued that this can be explained by only minor degassing (1–2%; Rowe and Schilling 1979). Interpreting the behavior of F in Icelandic basaltic magmas may also be complicated by crustal assimilation (Sigvaldason and Oskarsson 1986).

F degassing is reported to be negligible for Hawaiian magmas (~1%; Gerlach and Graeber 1985), although as in Iceland eruptions, minor F is present in eruption gases (e.g., Naughton et al. 1975). During Mauna Loa's last eruption in 1984, F was <1% of the sulfur content in eruption gases (Greenland 1987b). In our Mauna Loa glass suite, F correlates with K_2O (Fig. 3) and TiO_2, but with considerable scatter, as noted for Icelandic basalts (Sigvaldason and Oskarsson 1986). This scatter may be related in part to the relatively large analytical error for F (Fig. 3). In contrast to the behavior of S and Cl, there is no correlation of F or F/K_2O with sample collection

Table 2 Range and average of volatile concentrations and ratios in undegassed and uncontaminated tholeiitic glasses from the three active Hawaiian volcanoes. Glass compositions have been normalized to 7.0 wt% MgO by the subtraction of equilibrium composition olivine. See text for data sources and calculation methods. Lō'ihi Cl concentrations are minimum values. All values are in wt% except ratios

	Mauna Loa	Kilauea	Lō'ihi
SiO_2	51.5–52.7	50.5–51.5	48.5–50.1
S	0.096–0.149 (0.121)	0.090–0.124 (0.112)	0.12–0.17 (0.125)
F	0.027–0.042 (0.036)	0.035–0.040[a]	0.04–0.08 (0.05)
Cl	0.008–0.018 (0.012)	0.009–0.010[a]	0.020–0.022
Cl/K	0.029–0.055	0.022[a]	0.027–0.060
H_2O	0.38–0.46 (0.43)	0.55–0.75 (0.60)	0.41–0.60 (0.45)
H_2O/Ce	173–181[a]	180–200[a]	154–196

[a]Limited data

depth and some of the submarine glasses have lower F/K_2O than some of subaerial glasses (Figs. 5 and 8). Pillow rim glasses with S concentrations ranging from 0.02–0.10 wt% have comparable F/K_2O to glass inclusions (Fig. 8) and there is no correlation of F or F/K_2O with either H_2O or CO_2 (Tables 1 and 2; Fig. 7). However, a few glass inclusions have higher F/K_2O ratios; their origin is discussed in the next section.

We conclude from these results that F degassing is minor during subaerial and submarine Mauna Loa eruptions. This interpretation is consistent with the degassing behavior of basaltic lavas in laboratory studies in which F remains dissolved in melt even after H_2O and other volatiles are lost by degassing (Muenow et al. 1979) and with experimental work on synthetic melts (e.g., Lange 1994). The most likely explanation for the high solubility of F in basaltic magmas is its bonding with higher field-strength modifier cations (e.g., Al and Ca; Stebbins and Zeng 2000).

Crustal contamination of Mauna Loa lavas

Five to 10% of the submarine Mauna Loa pillow rim glasses and glass inclusions have elevated Cl contents (>0.025 wt%; Figs. 3 and 5). None of the Mauna Loa glasses have high F concentrations, but ~6% of the glass inclusions do. Even after normalizing halogen abundances to another highly incompatible element, K, to remove the effects of crystal fractionation, these halogen-rich glasses and glass inclusions remain anomalously high. For example, these glasses have Cl/K_2O ratios greater than 0.06, which is the upper limit for enriched MORB (Michael and Cornell 1998; Fig. 8). Surprisingly, some of the Cl-rich glasses have moderate to low S, H_2O, and CO_2 abundances (partially degassed), although most F-rich glass inclusions are S-rich (>800 ppm; Appendix 2). Although the two glass inclusions with the highest halogen concentration have elevated Cl and F concentrations, most of the inclusions with high Cl do not have high F, and vice versa. Similar results were reported for glass inclusions in five Hawaiian tholeiites (Hauri 2002). The presence of high halogen contents in olivine phenocryst-hosted glass inclusions argues that high halogen abundances are a magmatic feature and not a product of post-eruption alteration.

Elevated Cl contents are observed in submarine glasses from Kilauea and Lō'ihi (e.g., Clague et al. 1995; Kent et al. 1999a) and from mid-ocean ridges (e.g., Michael and Schilling 1989). In these cases, assimilation of a seawater-derived component was invoked to explain high Cl contents (e.g., Michael and Schilling 1989). In Hawaii, assimilation of seawater-modified rocks is thought to be most important for submarine volcanoes with ephemeral magma chambers (e.g., Lō'ihi; Kent et al. 1999a) rather than in mature volcanoes with a long-lived magma chamber (like Mauna Loa) that are thought to have dehydrated the surrounding crust and have freshwater-dominated circulating fluids (Dixon and Clague 2001). Also, seawater contamination cannot explain the high F concentration in some Mauna Loa glass inclusions. Therefore, some other source may be responsible for halogen-rich glasses.

Source heterogeneity was invoked to explain variable F abundances in glass inclusions in lavas from several Hawaiian volcanoes (Hauri 2002). However, this interpretation requires F to be more variable in the source than other volatiles, which is unlikely for Mauna Loa. Crustal contamination has been invoked to explain the high and variable F abundances in Icelandic lavas (Sigvaldason and Oskarsson 1986). Significant (7.5 to 84 wt%), but variable concentrations of F and Cl (Cl/F 2 to 1,000) are observed in Kilauea subaerial fumarole incrustations (Naughton et al. 1975). We propose that assimilation of such deposits is the most likely source for the high F concentrations in some Mauna Loa glass inclusions. It may also play a role in causing variable F/K_2O in the matrix glasses. High Cl content fumarole deposits (Naughton et al. 1975) may also be a source for the high Cl/K_2O observed in some glasses. However, the two Mauna Loa glasses with high Cl/K_2O (>0.07) and H_2O/K_2O (>1.3), but normal F/K_2O (<0.12), were probably contaminated by rocks containing saline brines (Fig. 10). Such contamination may also be partially responsible for high Cl in other glasses. Almost all of the halogen-rich glasses are from the submarine rift zone, so contamination probably occurs within the rift

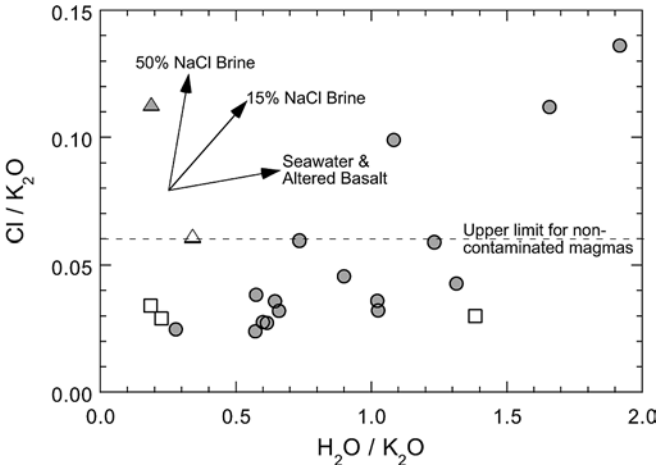

Fig. 10 Cl/K_2O versus H_2O/K_2O plot for Mauna Loa glasses. Arrows show the effects of various hydrous assimilants (modified from Kent et al. 1999a). High Cl/K_2O ratios can also be the product of contamination by hydrothermal deposits (see text for discussion). About 15% of these Mauna Loa glasses appear to have been contaminated

zone possibly in ephemeral magma bodies rather than in the summit magma chamber. These results demonstrate that contamination of magmas by seawater-derived components can occur after Hawaiian volcanoes emerge above sea level in contrast to predictions (Kent et al. 1999b).

The highly variable F/K_2O and Cl/K_2O in Mauna Loa glass inclusions in the same lava (Hauri 2002; Appendix 2) suggest that either uncontaminated magma is commonly mixed with contaminated magma, or crystals preferentially grow in marginal boundary layers that are more likely to be contaminated. Given that the extent of F enrichment is generally much less than for Cl enrichment in the glass inclusions (1.4–5 vs. 2.9–18; Fig. 8), it is easier to mask the effects of F contamination with the addition of new magma. This may explain why high F was observed in glass inclusions from the Laki eruption, but not in the erupted lavas (Thordarson et al. 1996).

Submarine radial vents of Mauna Loa Volcano

In 1877, there was a submarine radial vent eruption on Mauna Loa from vents at depths between 120 and 1,050 m b.s.l. (Fornari et al. 1980; Moore et al. 1985). Glasses from deeper vents (690 and 1,050 m b.s.l.) have high S contents (>1,000 ppm). We reanalyzed some of these glasses, which are strongly fractionated (MgO 5.9–6.0 wt%), and found 1,060–1,300 ppm S. Glasses from a shallow vent (~120 m b.s.l.) have lower S contents (~420 ppm; Fornari et al. 1980; Moore et al. 1985). In contrast, the glasses from the four radial vents we discovered in water depths between 1,200 and 2,000 m b.s.l. have very low S contents (63–174 ppm) and the one radial vent sample (M24-H) analyzed by FTIR has very low H_2O (~0.1 wt%) and CO_2 (<20 ppm). These low values typify subaerial eruptions. If these low values were caused by low pressure degassing at the vent site, at least 1,000 m of subsidence is required. This amount of subsidence is much greater than previously proposed for Mauna Loa's western flank (~400 m; Garcia et al. 1995b). If the regional subsidence rate for the island of Hawai'i of 2.5 mm/year (Moore et al. 1990) is used, the ages of these radial vents would have to be ~400 ka to allow for 1,000 m of subsidence. No surface Mauna Loa lava is known to be this old (e.g., Lipman et al. 1990). In addition, the presence of abundant fresh glass, hydrothermal deposits, and organisms at the vent sites implies they are young. Thus, we conclude that the lavas from these radial vents must have undergone low pressure degassing prior to eruption.

Moore et al. (1985) postulated that the 1877 radial vent submarine eruption was the result of tensional fractures associated with the Kealakekua fault tapping Mauna Loa's magma plumbing system. The northernmost of our new radial vents is in line with Kealakekua fault and, therefore, may have accessed the volcano's plumbing system using the same fracture system. Similarly, the southern radial vent lies at the head of a slump bench associated with the South Kona landslide (Moore et al. 1995) and the other radial vents are located near the Alika debris slide (Lipman et al. 1988) and the North Kona slump (Moore and Chadwick 1995). Thus, these magmas may also have followed tensional fractures related to these slides. However, unlike the 1877 eruption, the fractures for these older radial vents tapped degassed magma. Thus, the radial vents, like the southwest rift zone, are able to tap both degassed and undegassed magmas.

Volatile compositions of parental and primitive Mauna Loa magmas

High MgO glass inclusions are considered the best indicators of parental magma compositions (e.g., Roedder 1979; Kamenetsky and Clocchiatti 1996). Glass inclusions from our Mauna Loa suite have MgO contents up to 11.4 wt%, although the glasses with the highest MgO (>10 wt%) have anomalously low FeO (<8.5 wt%; Appendix 2). Low FeO is considered indicative of diffusion between the host olivine and the glass inclusion (Danyushevsky et al. 2000; Gaetani and Watson 2000). Other high MgO content (9.5–9.8 wt%), undegassed glass inclusions with normal FeO concentrations (>9.5 wt%) serve as good starting points to model parental volatile contents for Mauna Loa lavas. We also used the submarine rift glass with the highest MgO (7.9 wt%). The MELTS program (Ghiorso and Sack 1995) was used for crystal fractionation modeling to determine if these potential parental magma compositions produce liquid lines of descent that bracket the major element chemistry of most submarine and

subaerial glasses (Fig. 2). Modeling temperatures were based on the Mauna Loa empirical glass geothermometer of Montierth et al. (1995) and ranged between ~1,260 and 1,120 °C. The model starting parameters that gave the best fit for the major element variations were a pressure of 500 bar (consistent with a shallow magma chamber), oxygen fugacity buffer one log unit below QFM (consistent with values reported for Kilauea and Lō'ihi glasses; Byers et al. 1985; Wallace and Carmichael 1992) and an H_2O content of 0.1 wt% (which is at the lower limit of observed values and is representative of degassed lavas; Fig. 4). Models using higher water contents yielded lower incompatible element (K, P) abundances at a given MgO, although models with 0.3 wt% initial H_2O fit much of the data except the glasses with the highest incompatible abundances. This minor mismatch could be related to the inherent uncertainties of the MELTS program in modeling fractional crystallization or to magma chamber processes such as in situ crystallization (Langmuir 1989), or open system magmatism (periodically replenished, tapped and fractionated; O'Hara and Matthews 1981), which both cause incompatible element enrichment. Rhodes (1995) advocated open system processes, especially mixing involving distinct parental magmas, to explain the compositional variation for historical Mauna Loa magmas. In our suite of Mauna Loa lavas there is ample petrographic and olivine compositional data for magma mixing. However, the curved and kinked glass major element trends (Fig. 2) indicate that crystal fractionation is the dominant process affecting Mauna Loa magmas. Our modeling results indicate that the high MgO glasses are suitable parental magmas for most of the glasses we examined.

The high MgO glass inclusion and glass compositions were used to backtrack to primitive magma compositions by addition of equilibrium olivine compositions in 1-wt% steps. The volatiles are assumed to be highly incompatible (bulk partition coefficient $=0$) during crystal fractionation of olivine (e.g., Dixon and Clague 2001). Primitive Mauna Loa magma compositions are assumed to have at least 16 wt% MgO based on olivine–liquid equilibrium (Garcia et al. 1995b), which is consistent with some estimates for Kilauea (Clague et al. 1991, 1995). These calculations yield primitive magma compositions (16 wt% MgO) for the Mauna Loa high MgO glass inclusions of 860–1,160 ppm S, 95–105 ppm Cl, and 270–330 ppm F. The same procedures were used for the highest MgO glasses (with high H_2O/K_2O and low Cl) to estimate primitive magma H_2O contents from the pillow rim glasses, yielding values of 0.30–0.37 wt%. Using the same procedures (and data from Byers et al. 1985; Garcia et al. 1989; Clague et al. 1991, 1995; Dixon et al. 1991), Kilauea primitive magmas have comparable S, Cl, and F (900–1,000 ppm S, ~100 ppm Cl, ~300 ppm F), but higher H_2O (0.43–58 wt%) than those of Mauna Loa. Calculations for Lō'ihi tholeiitic primitive magmas yield H_2O, S, and F concentrations similar to Mauna Loa, but higher Cl (0.33–38 wt% H_2O, 620–1,320 ppm S, 300–400 ppm F and 130 to 220 ppm Cl; data from Byers et al. 1985; Garcia et al. 1989; Kent et al. 1999a; Dixon and Clague 2001). These calculations suggest that primitive magmas for these volcanoes have broadly similar volatile concentrations, but that Kilauea magmas have more H_2O and those from Lō'ihi have more Cl. A recent study of glass inclusions in Hawaiian tholeiites reached a similar conclusion, although it found that Kilauea magmas have less H_2O than those from Lō'ihi (Hauri 2002), in contrast to other more comprehensive studies of Kilauea and Lō'ihi glasses (Dixon et al. 1991; Dixon and Clague 2001). The volatile heterogeneity in the Hawaiian plume will be more thoroughly evaluated in the next section.

Volatile heterogeneity in the Hawaiian plume

Evidence is accumulating that the Hawaiian plume is heterogeneous in volatile concentrations and He isotopes, in addition to heavy isotopes (e.g., DePaolo et al. 2001; Dixon and Clague 2001). Volcanoes near the leading edge of the plume are thought to have higher volatile contents than those downstream from the core of the plume because volatiles are highly incompatible and concentrated in early formed magmas (Garcia et al. 1989; DePaolo et al. 2001). However, a recent study found that the source for Lō'ihi magmas at the leading edge of the Hawaiian plume have lower H_2O/Ce than the source for Kilauea magmas suggesting a relative depletion of H_2O in Lō'ihi's source (Dixon and Clague 2001).

To test the volatile zonation hypothesis for a large number of volatiles, we compared data for undegassed tholeiitic glasses from the three active Hawaiian volcanoes (Mauna Loa, Kilauea and Lō'ihi). Mauna Loa has passed over the plume and is now on the downstream side of the plume. Kilauea is located near the center of the Hawaiian plume and Lō'ihi is positioned close its leading edge (Rhodes and Hart 1995). Although all of these glasses are tholeiitic, they have distinct SiO_2 concentrations (Table 2) and melting histories (e.g., Clague et al. 1995; Garcia et al. 1995a, 2000; Rhodes and Hart 1995). The Mauna Loa glasses used in this study range in age from historical to ~250 ka. During this period, Mauna Loa lavas changed significantly in Pb, Sr, Nd, and He isotopes (Kurz et a. 1995; DePaolo et al. 2001), but there has been no systematic temporal change in ratios of major elements (Garcia et al. 1995b). Thus, the melting processes that control concentrations have not varied appreciably even though the mixture of source components has changed over the last 250 ka. Glasses that have evolved beyond olivine control (<6.7 wt% MgO) and those with evidence of crustal contamination were avoided for this comparison. We used ten glass inclusions and five pillow rim glasses to compute our

Mauna Loa range and average. The data sources for major elements and volatiles in Kilauea and Lō'ihi glasses are listed above. Glass compositions were normalized to 7.0 wt% MgO, a standard point of comparison for Hawaiian lavas (e.g., Clague et al. 1995), by subtraction of equilibrium olivine composition in 1-wt% steps, as discussed above.

Mauna Loa glasses have comparable S concentrations to those from Kilauea and Lō'ihi, although Lō'ihi glasses range to higher values (Table 2). F abundances are somewhat lower in Mauna Loa glasses than those from Loihi, but are compared with those from Kilauea (Table 2). Hauri (2002) reached similar conclusions from studying glass inclusions from one lava from each of these volcanoes and from compiling previous data.

Cl concentrations in Lō'ihi glasses at 7 wt% MgO are higher than those in glasses from Kilauea and Mauna Loa Volcanoes (Table 2). High Cl in Lō'ihi glasses have been explained by assimilation of Cl-bearing rocks (Kent et al. 1999). However, the Cl/K_2O ratios in the least contaminated Lō'ihi glasses are comparable with some Mauna Loa glasses (Table 2). Some Lō'ihi glasses have mantle hydrogen isotope values (Garcia et al. 1989). Thus, the high Cl in least contaminated Lō'ihi glasses is a result of their lower degree of partial melting compared to Kilauea and Mauna Loa (e.g., Garcia et al. 1995a; Dixon and Clague 2001) and not to a Cl-rich source.

H_2O concentrations in Mauna Loa glasses are similar to Lō'ihi, but distinctly lower than those in Kilauea magmas (0.38–0.46 vs. 0.55–0.75 wt%). Dixon and Clague (2001) found that H_2O was decoupled from major and incompatible trace elements and that its normalized abundance (H_2O/Ce) was not related to the extent or depth of melting. They proposed that one source component in the Hawaiian plume is H_2O-poor compared with the other source components, and they related this H_2O-poor component to dehydration of subducted oceanic crust during recycling in the deep mantle. This recycled ''Ko'olau'' component (e.g., Hauri 1996) is distinguished by relatively low $^{206}Pb/^{204}Pb$ and relatively high $^{87}Sr/^{86}Sr$. Based on isotopic compositions, Mauna Loa tholeiitic magmas generally contain a greater proportion of the ''Ko'olau'' component than Lō'ihi magmas (Kurz et al. 1995; Hauri 1996). H_2O/Ce values for two Mauna Loa glass samples (184-2 and 184-8) that do not appear to have been affected by either degassing or assimilation are 181 and 173 (Ce data from Garcia et al. 1995b). These H_2O/Ce ratios are within the range reported for Lō'ihi glasses (153–194). Thus, sources for Mauna Loa and Lō'ihi magmas have comparable H_2O, although Pb, Sr and Nd isotopic data indicate that they came from different mixtures of Hawaiian plume components (Kurz et al. 1995; Dixon and Clague 2001).

Recent ion probe work on melt inclusions from two Ko'olau Volcano samples found H_2O concentrations comparable to those of Mauna Loa (Hauri 2002). However, D/H ratios for Ko'olau melt inclusions indicate that its source underwent dehydration fractionation (possibly during subduction), which is consistent with the low S and Cl abundances in these inclusions (33% of glass inclusions from other Hawaiian volcanoes; Hauri 2002). In contrast, some submarine high-silica Ko'olau glasses have high S concentrations (850–1,200 ppm; Garcia 2002, unpublished data), so low S may not be diagnostic of Ko'olau magmas. Thus, the Ko'olau data do not show clear evidence for a volatile-poor component in the Hawaiian plume.

The inconsistent distribution of H_2O and Cl in glasses from three active volcanoes overlying the Hawaiian hotspot conflicts with the concentrically zoned plume model of Kurz et al. (1995) and DePaolo et al. (2001). Lō'ihi magmas contain high Cl, but not high H_2O, in contrast to the high H_2O but moderate Cl abundances in Kilauea magmas. Therefore, the simple concentrically zoned Hawaiian plume source model needs revision or mantle melting processes are able to decouple these elements. Work is in progress on volatiles in Mauna Kea volcano glasses (Seaman et al. in review). This volcano is similar to Kilauea in its source composition and to its location on the edge of the plume at the time of formation (e.g., DePaolo et al. 2001) and thus will help resolve the source heterogeneity option.

Conclusions

Most Mauna Loa submarine rocks we collected, including those from depths >1 km, are pillow lavas with low S contents (<300 ppm) glasses. The low S concentrations of these submarine glasses are identical to subaerially erupted glasses, which indicate that they underwent low pressure degassing before quenching. These results imply that most of the volcano's submarine flank is covered with subaerially erupted pillow lavas that must have crossed the shoreline or that lavas drained back into the volcano and were re-erupted, as observed for the newly discovered radial vents. These results support the model that pillow lava is the dominant rock type within ocean island volcanoes.

The newly discovered submarine radial vents on the western flank of Mauna Loa are young cones that postdate the large landslides that occurred in the same region. These vents may be related to faults, such as the Kealakekua fault, and slump structures. However, unlike the Mauna Loa radial vent eruption of 1877, these vents produced degassed magmas.

In contrast, many rift zone glasses are undegassed or only partially degassed and show an increase in both maximum S and Cl with depth along the rift. The partially degassed glasses have variable S, H_2O, Cl, and CO_2 and were collected at depths where S and H_2O should have remained dissolved in the magma. These results are identical to those reported for Kilauea's east

rift zone and support a model of mixing between undegassed and degassed components within the rift.

Elevated F and Cl concentrations indicate that crustal contamination has affected 5–10% of Mauna Loa magmas, especially those erupted along the submarine rift zone. Contamination may occur by assimilation of high-temperature fumarole deposits and rocks that have exchanged with seawater, perhaps while the magmas resided in ephemeral magma chambers within the submarine rift zone.

F degassing appears to be negligible for both subaerial and submarine Mauna Loa eruptions.

Primitive magma volatile concentrations were constrained by modeling high MgO (>9.5 wt%) glass inclusions. At ~16 wt% MgO, the modeling indicates that Mauna Loa magmas had ~0.30 wt% H_2O, ~860 to 1,160 ppm S, 95 to 105 ppm Cl, and between 270 to 330 ppm F. These concentrations are similar to those for glasses from Kilauea and Lō'ihi Volcanoes except H_2O is lower for Mauna Loa and Lō'ihi and Cl is higher for Lō'ihi glasses. Comparing volatile contents for a larger group of glasses from the three active Hawaiian volcanoes normalized to 7.0 wt% MgO, Kilauea magmas are found to have significantly higher H_2O contents compared with both Mauna Loa and Lō'ihi. The sources for Lō'ihi and Mauna Loa have similar Cl/K_2O ratios, so the higher Cl content of Lō'ihi glasses is related to lower degrees of partial melting. The dissimilar distribution of H_2O and Cl, two highly incompatible components, seems inconsistent with the simple zoned plume model.

Acknowledgments Thanks to the captain, crew, and the intrepid science team of R/V *Moana Wave* 1999 Gale Force cruise. Mahalo to Cliff Todd for help with numerous microprobe questions, J. Michael Rhodes for glassy Mauna Loa subaerial samples, Eric DeCarlo for identifying the Mn mineral todorokite in our radial vent samples, P. Cervantes and C. Petko for assistance with sample preparation and FTIR spectroscopy, to Sarah Sherman and Peter Michael for discussions on volatiles and help with volatile analysis, and to Jackie Dixon and Leonid Danyushevsky for helpful reviews of the manuscript.

Appendix 1

Microprobe analyzes of major and volatile element compositions (in wt%) of glasses from different morphological regions of Mauna Loa. Elevations (*elev.*) are in meters; submarine elevations (–) are minimum dredge depths (except samples 182–185, which are dive depths). Total iron is given as FeO

Sample	Elev.	SiO_2	TiO_2	Al_2O_3	FeO	MnO	MgO	CaO	Na_2O	K_2O	P_2O_5	S	Cl	F	Sum
Subaerial rift zone															
ML-129	4,054	52.43	2.10	13.75	11.10	0.17	6.58	10.72	2.34	0.39	0.24	0.0127	0.0091	0.0328	99.86
ML-80	3,962	52.55	2.16	13.94	10.76	0.16	6.61	10.69	2.36	0.48	0.28	0.0110	0.0104	0.0422	100.06
ML-288	3,810	52.62	2.71	13.11	12.26	0.21	5.36	10.10	2.52	0.56	0.29	0.0126	0.0096	0.0397	99.81
ML-261	3,353	52.44	2.14	13.91	10.90	0.21	6.28	10.65	2.41	0.41	0.23	0.0095	0.0119	0.0260	99.65
ML-45	3,246	52.84	2.18	13.58	11.11	0.15	6.27	10.68	2.35	0.38	0.22	0.0136	0.0106	0.0355	99.82
ML-274	2,658	52.63	2.17	13.76	11.13	0.18	6.27	10.73	2.36	0.40	0.27	0.0151	0.0082	0.0341	99.95
ML-52	2,627	52.46	2.75	13.02	12.42	0.22	5.46	10.07	2.49	0.60	0.35	0.0098	0.0107	0.0474	99.90
ML-284	2,588	52.61	2.49	13.53	11.56	0.21	5.79	10.30	2.20	0.56	0.27	0.0164	0.0113	0.0431	99.60
ML-37	2,195	52.13	2.34	13.32	12.02	0.20	5.94	10.41	2.37	0.44	0.26	0.0185	0.0117	0.0367	99.48
ML-91	1,829	52.66	2.44	13.36	12.06	0.17	5.90	10.40	1.99	0.43	0.32	0.0373	0.0113	0.0377	99.82
ML-93	1,814	52.78	2.16	13.62	11.32	0.19	6.39	10.61	2.33	0.38	0.22	0.0146	0.0105	0.0297	100.07
ML-8	1,600	52.61	2.00	13.94	10.61	0.18	6.63	10.55	2.26	0.40	0.25	0.0210	0.0079	0.0368	99.50
ML-7	1,400	52.54	2.30	13.60	11.91	0.23	5.92	10.42	2.26	0.39	0.25	0.0112	0.0099	0.0381	99.89
ML-6a	1,360	52.52	2.12	14.13	11.06	0.15	6.50	10.73	1.91	0.40	0.25	0.0057	0.0076	0.0421	99.85
ML-6	1,360	52.61	2.55	13.68	11.58	0.19	5.65	10.07	2.52	0.58	0.34	0.0068	0.0103	0.0527	99.85
ML-37	930	52.56	2.20	13.91	10.70	0.19	6.81	10.61	1.98	0.43	0.25	0.0075	0.0081	0.0404	99.71
ML-2	900	52.16	1.97	13.62	10.79	0.18	7.81	10.47	2.20	0.37	0.23	0.0196	0.0064	0.0398	99.85
ML-1	840	52.37	2.15	13.85	10.61	0.21	6.80	10.73	2.24	0.41	0.28	0.0102	0.0094	0.0391	99.70
ML-88	610	52.65	2.26	13.78	10.78	0.17	6.48	10.73	2.30	0.45	0.26	0.0076	0.0082	0.0374	99.90
ML-5	180	51.90	2.15	13.83	11.18	0.17	6.81	10.97	2.22	0.34	0.21	0.0106	0.0089	0.0308	99.84
ML-5a	170	52.16	2.15	13.81	10.97	0.18	6.72	10.96	2.26	0.34	0.23	0.0103	0.0083	0.0331	99.82
Submarine rift zone															
M19-02	–500	52.39	2.25	13.94	10.14	0.18	6.83	10.89	2.21	0.41	0.23	0.0418	0.0148	0.0407	99.57
M19-05	–500	51.96	2.09	13.91	9.89	0.14	6.73	10.91	2.29	0.33	0.21	0.071	0.0099	0.0321	98.58
M19-11	–500	52.39	2.09	14.17	9.78	0.17	6.88	10.97	2.29	0.33	0.18	0.0740	0.0118	0.0326	99.35
184-11	–745	52.01	2.54	13.60	10.68	0.18	6.26	10.30	2.23	0.40	0.23	0.0131	0.0097	0.0264	98.47
184-9	–775	51.91	2.12	13.99	10.42	0.15	7.01	11.11	2.21	0.31	0.20	0.0472	0.0111	0.0275	99.51
184-8	–1,020	52.19	2.32	13.66	11.78	0.18	6.24	10.63	2.43	0.38	0.18	0.1134	0.0123	0.0310	100.14
183-3	–1,110	52.03	2.00	13.45	10.30	0.19	8.24	10.47	2.10	0.30	0.18	0.0395	0.0137	0.0182	99.34
182-7	–1,265	51.28	2.17	13.41	10.52	0.15	8.42	10.70	2.16	0.33	0.183	0.0575	0.0200	0.0261	99.44
182-6	–1,310	51.51	2.17	13.45	10.36	0.15	8.26	10.75	2.21	0.34	0.183	0.0561	0.0202	0.0264	99.48
182-3	–1,395	50.83	2.32	14.06	10.21	0.22	6.72	11.12	2.62	0.23	0.206	0.0390	0.0138	0.0262	98.60
185-11	–1,505	51.95	2.81	13.28	12.10	0.16	6.09	10.39	2.34	0.44	0.26	0.0641	0.0108	0.0321	99.92

Appendix 1 (Contd.)

185-10	–1,515	52.28	2.70	13.54	12.03	0.21	6.03	10.00	2.45	0.42	0.27	0.0582	0.0101	0.0299	100.02
184-5	–1,535	52.06	2.11	14.01	10.20	0.16	6.95	11.22	2.29	0.32	0.20	0.0778	0.0114	0.0218	99.63
185-7a	–1,620	52.50	2.51	13.71	11.46	0.18	6.22	9.89	2.47	0.38	0.22	0.0561	0.0097	0.0299	99.63
185-6a	–1,655	52.43	2.61	13.89	10.81	0.15	6.29	9.95	2.41	0.47	0.32	0.0713	0.0157	0.0408	99.45
185-4	–1,700	52.35	2.70	13.88	11.25	0.17	6.23	10.22	2.39	0.51	0.29	0.0682	0.0153	0.0417	100.11
184-2	–1,735	51.81	2.01	13.73	10.49	0.16	7.90	10.90	2.18	0.30	0.18	0.0957	0.0177	0.0265	99.80
185-3	–1,735	52.45	2.80	13.62	11.50	0.19	5.84	9.71	2.52	0.50	0.34	0.0589	0.0138	0.0422	99.58
185-2	–1,795	52.40	2.85	13.55	11.53	0.19	5.91	9.88	2.54	0.50	0.28	0.0764	0.0160	0.0484	99.77
185-1	–1,825	52.67	2.71	13.57	11.46	0.17	6.20	10.03	2.49	0.44	0.27	0.0729	0.0158	0.0411	100.14
ML1-11	–1,925	52.46	2.20	14.21	9.91	0.18	6.39	11.50	2.28	0.34	0.250	0.0641	0.0105	0.0247	99.82
ML1-10	–1,925	52.38	2.83	13.58	11.05	0.19	6.01	9.86	2.49	0.52	0.330	0.0856	0.0166	0.0444	99.39
ML1-12	–1,925	52.43	2.15	14.09	10.01	0.19	6.70	11.12	2.32	0.35	0.230	0.0644	0.0117	0.0260	99.70
ML2-8	–1,950	52.04	2.01	13.94	9.91	0.17	7.65	10.88	2.23	0.32	0.230	0.0628	0.0144	0.0228	99.48
ML4-11	–1,975	51.95	2.67	13.80	11.38	0.19	6.05	10.40	2.44	0.48	0.310	0.0680	0.0143	0.0435	99.80
ML4-10	–1,975	52.04	2.01	13.89	10.35	0.18	7.63	10.82	2.26	0.33	0.260	0.0649	0.0135	0.0248	99.87
ML1-11	–1,925	52.46	2.20	14.21	9.91	0.18	6.39	11.50	2.28	0.34	0.250	0.0641	0.0105	0.0247	99.82
M18-01	–2,600	52.39	2.41	13.58	11.15	0.17	6.36	10.44	2.33	0.39	0.27	0.0134	0.0184	0.0352	99.54
M18-02	–2,600	52.40	2.41	13.65	11.15	0.19	6.39	10.46	2.37	0.41	0.27	0.0147	0.0190	0.0437	99.76
M18-16	–2,600	52.73	2.19	14.16	9.88	0.17	6.83	10.86	2.27	0.35	0.22	0.0136	0.0102	0.0427	99.72
M1-02	–3,000	51.86	2.14	13.75	11.27	0.20	6.50	10.89	2.36	0.41	0.24	0.0619	0.0112	0.0429	99.73
M1-03	–3,000	51.74	2.06	14.09	10.83	0.20	6.30	10.98	2.36	0.38	0.24	0.0769	0.0113	0.0481	99.31
M1-06	–3,000	51.52	2.06	14.06	10.69	0.20	6.54	11.01	2.34	0.38	0.24	0.0525	0.0104	0.0402	99.14
M1-08	–3,000	52.29	2.11	13.94	10.10	0.20	6.86	10.95	2.27	0.33	0.20	0.0261	0.0206	0.0376	99.35
M1-13a	–3,000	52.50	2.00	13.30	10.11	0.20	7.91	11.34	2.11	0.31	0.19	0.1218	0.0112	0.0396	100.13
M1-13b	–3,000	52.38	2.01	13.96	10.11	0.20	6.86	10.86	2.19	0.31	0.18	0.1218	0.0112	0.0396	99.23
M1-16	–3,000	52.01	1.90	14.22	9.94	0.20	7.41	11.23	2.26	0.30	0.18	0.0955	0.0086	0.0365	99.78
M1-17	–3,000	52.24	1.92	14.01	9.86	0.20	7.44	10.89	2.23	0.29	0.18	0.0751	0.0086	0.0415	99.39
M2-02	–3,000	52.15	2.25	14.23	10.02	0.20	6.48	10.96	2.32	0.33	0.21	0.0516	0.0479	0.0322	99.28
M2-03	–3,000	51.97	2.24	13.91	10.31	0.20	6.87	10.85	2.22	0.35	0.20	0.0658	0.0476	0.0330	99.27
M2-04	–3,000	51.73	2.22	13.83	10.21	0.20	7.19	10.75	2.28	0.35	0.18	0.0625	0.0426	0.0315	99.08
M2-05	–3,000	52.15	2.26	14.09	9.98	0.20	6.44	10.94	2.29	0.36	0.20	0.0724	0.0356	0.0294	99.05
M2-06	–3,000	51.75	2.20	13.86	10.14	0.20	7.05	10.76	2.31	0.36	0.20	0.0703	0.0380	0.0330	98.98
M2-07	–3,000	52.38	2.14	14.04	10.08	0.20	6.81	10.84	2.32	0.34	0.19	0.0761	0.0121	0.0407	99.46
M2-08	–3,000	52.13	2.24	13.94	10.12	0.20	6.84	10.87	2.34	0.34	0.20	0.0710	0.0292	0.0332	99.36
M2-17	–3,000	51.99	2.21	13.91	10.46	0.20	7.02	10.83	2.22	0.34	0.19	0.0724	0.0343	0.0358	99.51
M3-01	–3,700	51.99	2.40	14.95	11.43	0.20	5.41	10.37	2.58	0.42	0.21	0.1121	0.0388	0.0354	100.15
M3-02	–3,700	52.03	2.64	13.70	11.43	0.20	5.49	9.75	2.39	0.44	0.25	0.1422	0.0493	0.0395	98.56
M4-01	–4,000	52.74	2.40	14.00	10.35	0.20	6.75	10.68	2.35	0.37	0.17	0.0559	0.0106	0.0467	100.11
M4-03	–4,000	52.20	2.28	13.94	10.38	0.20	7.34	10.87	2.30	0.35	0.18	0.0659	0.0133	0.0329	100.14
M4-06	–4,000	52.41	2.29	13.88	10.22	0.20	7.32	10.94	2.33	0.35	0.17	0.0632	0.0187	0.0395	100.24
M4-08	–4,000	52.41	2.30	13.97	10.26	0.20	7.29	10.89	2.32	0.35	0.17	0.0658	0.0142	0.0358	100.26
M4-10	–4,000	52.38	2.31	14.01	10.28	0.20	7.07	10.96	2.33	0.35	0.19	0.0623	0.0157	0.0408	100.20
M4-11	–4,000	51.53	2.23	13.86	10.14	0.20	6.59	10.42	2.35	0.35	0.16	0.1269	0.0150	0.0369	98.02
M4-13	–4,000	52.11	2.26	13.76	10.54	0.20	7.47	10.70	2.35	0.35	0.17	0.0692	0.0151	0.0323	100.03
Submarine flank															
M16-11	–1,000	52.20	2.54	13.45	10.70	0.19	6.13	10.37	2.49	0.42	0.29	0.0103	0.0089	0.0329	98.85
M16-15	–1,000	51.73	2.82	13.13	11.85	0.19	5.57	10.17	2.48	0.45	0.29	0.0111	0.0108	0.0457	98.76
M16-23	–1,000	51.79	2.69	12.43	11.76	0.21	6.62	10.40	2.32	0.41	0.26	0.0104	0.0091	0.0457	98.94
M16-24	–1,000	51.51	2.92	12.55	13.20	0.25	5.16	9.63	2.66	0.60	0.37	0.0116	0.0111	0.0584	98.91
M16-34	–1,000	52.33	2.39	13.94	10.16	0.14	6.22	10.65	2.45	0.42	0.26	0.0102	0.0133	0.0285	99.01
M17-03	–1,000	52.68	2.35	13.61	10.72	0.15	6.52	10.70	2.36	0.37	0.20	0.0175	0.0103	0.0378	99.72
M17-04	–1,000	52.53	2.60	13.34	11.14	0.19	6.14	10.23	2.45	0.43	0.27	0.0064	0.0088	0.0374	99.38
M17-05	–1,000	52.53	2.67	13.40	11.41	0.17	6.02	10.18	2.46	0.42	0.28	0.0084	0.0097	0.0485	99.60
M17-06	–1,000	51.79	2.25	13.74	10.55	0.17	6.75	10.62	2.39	0.36	0.23	0.0129	0.0096	0.0378	98.90
M17-07	–1,000	51.86	2.17	13.68	10.14	0.17	7.08	10.91	2.26	0.33	0.21	0.0131	0.0081	0.0288	98.86
M25-01	–1,700	52.25	2.93	13.16	11.96	0.19	5.88	10.15	2.45	0.48	0.32	0.0103	0.0120	0.0378	99.83
M15-33	–2,400	51.96	2.42	13.06	11.80	0.19	5.75	10.07	2.40	0.48	0.31	0.0154	0.0176	0.0485	98.53
M15-34	–2,400	52.17	2.40	13.35	11.70	0.18	5.96	10.12	2.38	0.47	0.33	0.0176	0.0187	0.0514	99.14
M15-52	–2,400	51.94	2.44	13.11	11.78	0.19	5.80	10.07	2.40	0.48	0.30	0.0156	0.0165	0.0498	98.61
M15-53	–2,400	52.30	2.36	13.66	11.64	0.18	5.93	10.14	2.41	0.48	0.30	0.0133	0.0178	0.0359	99.46
M26-08	–2,500	52.72	2.23	13.85	10.64	0.19	6.64	10.63	2.32	0.36	0.24	0.0265	0.0074	0.0313	99.88
M26-12	–2,500	51.86	2.59	13.23	11.78	0.18	5.62	10.10	2.60	0.52	0.31	0.0202	0.0148	0.0457	98.86
M26-14	–2,500	52.08	2.12	13.84	10.25	0.18	6.65	10.48	2.33	0.35	0.23	0.0421	0.0105	0.0429	98.62
M26-15	–2,500	52.07	2.14	13.59	10.48	0.18	6.50	10.59	2.37	0.34	0.22	0.0386	0.0116	0.0335	98.57
M26-19	–2,500	52.62	2.14	13.88	10.58	0.16	6.73	10.72	2.33	0.33	0.19	0.0384	0.0124	0.0377	99.76
M26-34	–2,500	52.52	2.15	13.89	10.32	0.18	6.65	10.75	2.37	0.35	0.21	0.0372	0.0123	0.0313	99.47
M26-35	–2,500	52.50	2.55	13.42	11.62	0.20	5.89	10.12	2.51	0.50	0.27	0.0180	0.0186	0.0446	99.65

Appendix 1 (Contd.)

M8-01	–2,700	51.56	2.49	13.41	11.73	0.22	5.89	10.42	2.43	0.43	0.29	0.0098	0.0126	0.0297	98.92
M8-02	–2,700	51.87	2.78	13.60	12.67	0.19	5.57	10.03	2.49	0.44	0.24	0.0098	0.0134	0.0349	99.94
M6-10	–3,000	51.79	3.15	12.74	12.91	0.20	5.23	9.65	2.48	0.47	0.27	0.0183	0.0121	0.0503	98.96
M6-25	–3,000	51.47	2.94	12.94	12.70	0.19	5.41	9.67	2.53	0.51	0.35	0.0178	0.0173	0.0533	98.80
M6-31	–3,000	51.82	3.09	12.68	12.99	0.24	5.37	9.70	2.42	0.49	0.30	0.0168	0.0122	0.0404	99.17
M29-01	–3,100	52.57	2.50	13.66	11.35	0.18	6.32	10.37	2.32	0.38	0.24	0.0203	0.0329	0.0372	99.97
M29-04	–3,100	52.47	2.42	13.79	10.46	0.17	6.40	10.65	2.35	0.37	0.19	0.0228	0.0210	0.0303	99.36
M29-05	–3,100	52.66	2.47	13.65	11.40	0.20	6.27	10.41	2.35	0.41	0.28	0.0207	0.0315	0.0402	100.19
M30-01	–3,100	52.69	2.19	14.07	9.72	0.18	6.62	10.60	2.28	0.34	0.26	0.1297	0.0102	0.0324	99.13
M30-03	–3,100	52.16	2.27	13.53	10.97	0.17	6.53	10.75	2.26	0.33	0.22	0.0048	0.0079	0.0335	99.23
Landslide debris															
M13-04	–4,000	52.13	2.30	13.79	10.36	0.15	6.30	10.68	2.45	0.42	0.26	0.0105	0.0157	0.0339	98.91
M13-09	–4,000	52.52	2.18	13.47	10.84	0.19	6.61	10.77	2.24	0.33	0.18	0.0040	0.0087	0.0283	99.36
M14-01	–4,000	51.60	2.12	13.76	10.12	0.15	7.10	10.96	2.33	0.34	0.21	0.0041	0.0131	0.0262	98.73
M14-04	–4,000	52.01	2.18	13.84	10.14	0.20	6.97	11.08	2.18	0.33	0.20	0.0035	0.0117	0.0340	99.16
M14-05	–4,000	51.88	2.15	13.66	10.60	0.15	6.48	11.05	2.28	0.33	0.21	0.0063	0.0095	0.0242	98.84
M14-08	–4,000	51.88	2.15	14.04	10.72	0.18	5.99	11.05	2.29	0.32	0.19	0.0083	0.0198	0.0286	98.87
M14-14	–4,000	51.83	2.13	13.86	9.93	0.13	6.89	10.98	2.22	0.32	0.23	0.0032	0.0105	0.0312	98.57
Radial vents															
ML-295	3,365	52.40	2.37	13.80	10.71	0.17	6.03	10.62	2.46	0.46	0.24	0.0072	0.0087	0.0410	99.30
ML-300	2,865	52.30	2.15	13.92	10.87	0.18	7.07	10.71	1.66	0.43	0.26	0.0131	0.0079	0.0442	99.62
M28-01	–1,200	52.15	2.65	13.02	12.83	0.19	5.50	9.97	2.50	0.50	0.30	0.0137	0.0116	0.0460	99.69
M28-10	–1,200	51.66	2.70	12.77	12.90	0.21	5.29	9.84	2.57	0.53	0.32	0.0126	0.0114	0.0498	98.87
M28-11	–1,200	52.29	2.67	12.97	12.87	0.22	5.54	9.91	2.47	0.53	0.30	0.0127	0.0119	0.0481	99.84
M28-14	–1,200	52.19	2.66	13.00	12.91	0.19	5.54	9.94	2.46	0.54	0.30	0.0138	0.0095	0.0484	99.79
M28-21	–1,200	52.16	2.36	13.63	10.17	0.22	6.62	10.99	2.38	0.40	0.28	0.0158	0.0100	0.0320	99.26
M24-01	–1,600	52.71	2.35	13.80	10.65	0.18	6.36	10.54	2.35	0.48	0.31	0.0095	0.0082	0.0493	99.80
M24-A	–1,600	52.55	2.30	13.76	10.75	0.18	6.36	10.67	2.36	0.48	0.25	0.0093	0.0087	0.0475	99.72
M24-E	–1,600	52.90	2.35	13.71	10.89	0.18	6.38	10.63	2.42	0.49	0.29	0.0174	0.0562	0.0498	100.37
M24-G	–1,600	52.67	2.33	13.84	10.78	0.17	6.45	10.62	2.40	0.47	0.27	0.0105	0.0079	0.0464	100.07
M24-H	–1,600	52.75	2.31	13.76	10.76	0.19	6.40	10.65	2.41	0.48	0.26	0.0173	0.0543	0.0479	100.09
M24-I	–1,600	52.72	2.32	13.75	10.83	0.20	6.37	10.61	2.38	0.46	0.29	0.0090	0.0091	0.0477	100.00
M27-01	–1,600	51.59	2.48	13.43	11.69	0.20	6.28	10.82	2.38	0.44	0.29	0.0132	0.0124	0.0473	99.65
M27-02	–1,600	51.75	2.48	13.48	11.51	0.21	6.29	10.85	2.37	0.43	0.26	0.0141	0.0089	0.0331	99.68
M27-11	–1,600	51.60	2.45	13.40	11.54	0.17	6.25	10.75	2.41	0.44	0.28	0.0126	0.0111	0.0328	99.36
M27-12	–1,600	51.50	2.49	13.49	11.91	0.16	6.29	10.85	2.43	0.43	0.30	0.0139	0.0091	0.0449	99.91
M27-28	–1,600	52.38	2.47	13.55	10.26	0.14	6.31	10.82	2.40	0.40	0.30	0.0085	0.0116	0.0348	99.10
M27-37	–1,600	52.76	2.21	13.76	10.39	0.19	6.49	10.61	2.46	0.44	0.23	0.0063	0.0077	0.0294	99.57
M22-04	–1,700	52.69	2.37	14.06	9.94	0.18	6.79	10.77	2.37	0.39	0.23	0.0112	0.0127	0.0298	99.86
M22-11	–1,700	52.11	2.49	13.74	10.51	0.18	6.33	10.62	2.48	0.40	0.27	0.0109	0.0145	0.0360	99.19

Appendix 2

Microprobe analyses of major and volatile element compositions (in wt%) of olivine-hosted glass inclusions from Mauna Loa's submarine southwest rift zone. Total iron given as FeO. The superscript a denotes samples that have been affected by post-entrapment Fe exchange. *H* Samples that were heated (see text for explanation); *m* matrix

Sample	SiO_2	TiO_2	Al_2O_3	FeO	MnO	MgO	CaO	Na_2O	K_2O	P_2O_5	S	Cl	F	Sum
ML1-11-7a[a]	52.51	1.91	13.87	7.42	0.11	11.06	10.35	2.08	0.26	0.20	0.0992	0.0086	0.0447	99.91
ML2-8-11	51.83	2.23	13.76	9.12	0.17	6.93	11.62	2.13	0.34	0.25	0.1069	0.0109	0.0429	98.52
ML2-8-21	51.81	2.06	13.55	10.22	0.20	6.79	11.37	2.11	0.31	0.21	0.0527	0.0141	0.0668	98.77
ML4-10-29	50.03	2.09	13.41	10.19	0.15	9.54	10.53	2.15	0.31	0.23	0.1393	0.0128	0.0394	98.81
ML4-10-30	51.76	2.15	13.74	10.53	0.20	6.02	11.73	2.12	0.30	0.20	0.1390	0.0132	0.1642	99.06
182-6b-52a[a]	51.65	2.18	13.32	8.75	0.14	8.12	11.13	2.10	0.35	0.21	0.1134	0.1753	0.2240	98.47
182-6b-22[a]	52.06	2.01	13.67	8.75	0.16	8.01	11.05	2.09	0.31	0.17	0.0780	0.0063	0.0196	98.39
182-6b-57	51.15	2.18	13.11	10.25	0.12	8.01	10.39	2.19	0.32	0.21	0.0946	0.0176	0.0301	98.09
182-6b-63[a]	51.60	2.28	13.55	8.90	0.22	7.99	10.98	2.17	0.38	0.35	0.1422	0.0104	0.0306	98.60
182-6b-9	50.92	2.17	13.23	10.58	0.25	7.95	10.48	2.20	0.29	0.17	0.0574	0.0158	0.0343	98.34
182-6b-66a	51.16	2.14	13.02	10.40	0.17	7.82	10.61	2.17	0.34	0.29	0.0609	0.0197	0.0282	98.24
182-6b-19	51.31	2.23	12.83	11.07	0.14	7.79	10.58	2.03	0.25	0.23	0.0974	0.0098	0.0317	98.60
182-6b-6b	51.42	2.10	13.51	9.46	0.21	7.78	11.04	2.01	0.29	0.21	0.1427	0.0200	0.0362	98.24
182-6b-72	51.48	2.34	13.40	9.02	0.22	7.66	11.41	2.03	0.34	0.28	0.1048	0.0103	0.0300	98.31

Appendix 2 (Contd.)

182-6b-36a	49.71	2.35	12.76	12.32	0.14	7.64	10.58	1.97	0.35	0.32	0.1337	0.0106	0.0307	98.31
182-6b-48b[a]	52.16	2.29	13.60	8.47	0.14	7.63	11.15	2.19	0.39	0.14	0.1423	0.0100	0.0303	98.35
182-6b-31b[a]	51.52	2.32	13.41	8.85	0.17	7.62	11.61	2.05	0.35	0.20	0.0420	0.0047	0.0091	98.16
182-6b-29	50.97	2.12	13.15	10.83	0.25	7.44	11.00	2.02	0.33	0.29	0.0859	0.0166	0.0318	98.54
182-6b-33c	51.17	2.10	13.14	10.69	0.17	7.30	11.19	2.10	0.35	0.30	0.0274	0.0091	0.0128	98.57
182-6b-65[a]	51.86	2.27	14.07	8.05	0.22	7.29	11.83	2.12	0.28	0.17	0.0065	0.1017	0.0156	98.28
182-6b-16	50.95	2.10	13.32	11.18	0.13	6.63	11.87	1.95	0.29	0.22	0.1275	0.0103	0.0442	98.83
182-6b-64	51.25	2.14	13.16	10.78	0.22	6.54	11.42	2.13	0.29	0.16	0.0080	0.0608	0.0066	98.15
182-6b-33b	51.48	1.91	14.53	10.55	0.19	5.61	10.69	2.18	0.38	0.24	0.0202	0.1153	0.0255	97.93
183-11-16[a]	52.60	2.05	14.10	6.44	0.15	11.43	10.60	2.05	0.18	0.30	0.0170	0.0185	0.0154	99.95
183-3-40	50.86	1.94	13.89	10.16	0.17	9.77	10.45	2.10	0.36	0.18	0.1248	0.0127	0.0334	100.05
183-3-67	51.89	2.06	13.38	10.42	0.20	8.03	10.68	2.17	0.31	0.19	0.0917	0.0096	0.0312	99.45
183-3-181	51.65	2.00	13.36	10.11	0.11	7.98	10.85	2.11	0.31	0.19	0.1301	0.0087	0.0367	98.84
183-3-9	51.56	2.04	13.14	10.23	0.13	7.84	11.61	2.14	0.30	0.18	0.0757	0.0090	0.0345	99.29
183-3-199	51.61	2.05	13.31	10.78	0.18	7.71	11.07	2.11	0.30	0.21	0.0391	0.0140	0.0300	99.42
183-3-39	51.66	1.94	13.50	10.09	0.15	7.70	11.14	2.12	0.31	0.28	0.1170	0.0063	0.0309	99.03
183-3-22b	51.71	2.05	13.18	10.54	0.16	7.68	10.85	2.13	0.31	0.19	0.0406	0.0111	0.0236	98.88
183-3-22a	51.49	2.04	13.27	10.55	0.17	7.65	10.99	2.12	0.31	0.19	0.0382	0.0129	0.0284	98.85
183-3-157	51.79	2.07	13.38	10.68	0.18	7.62	10.92	2.05	0.30	0.19	0.0396	0.0108	0.0244	99.25
183-3-190	51.53	2.04	13.20	10.82	0.18	7.58	11.14	2.07	0.30	0.23	0.0404	0.0102	0.0346	99.17
183-3-59	51.81	2.08	13.49	10.66	0.20	7.44	11.13	2.09	0.30	0.16	0.0803	0.0106	0.0404	99.49
183-3-93	51.60	2.10	13.27	10.79	0.18	7.40	11.25	2.09	0.30	0.22	0.0511	0.0139	0.0261	99.28
183-3-194	51.77	2.11	13.25	11.06	0.20	7.36	11.27	2.05	0.28	0.22	0.0474	0.0151	0.0333	99.68
183-3-192	51.82	2.09	13.39	10.93	0.20	7.33	11.16	2.07	0.29	0.22	0.0410	0.0119	0.0299	99.57
183-3-14	51.84	2.08	13.30	10.80	0.17	7.30	11.34	2.04	0.29	0.21	0.0418	0.0120	0.0327	99.45
183-3-121	51.75	2.11	13.49	10.66	0.18	7.29	11.46	2.03	0.30	0.19	0.0463	0.0179	0.0364	99.56
183-3-145	51.63	2.15	13.79	10.02	0.19	7.26	11.71	2.02	0.29	0.23	0.0760	0.0078	0.0440	99.41
183-3-50	51.44	1.97	13.53	10.45	0.16	6.98	11.62	2.04	0.32	0.22	0.1328	0.0082	0.0243	98.89
183-3-164	52.03	2.08	13.51	10.83	0.19	6.94	11.41	2.02	0.29	0.19	0.0899	0.3653	0.0567	99.99
183-3-96	51.60	2.04	13.29	10.86	0.20	6.92	11.57	2.02	0.27	0.22	0.0470	0.0113	0.0309	99.06
183-3-21	52.00	2.13	13.53	10.36	0.18	6.90	11.56	2.06	0.29	0.22	0.0395	0.0107	0.0330	99.31
183-3-140	51.68	2.03	13.28	11.31	0.15	6.89	11.33	2.05	0.27	0.19	0.1394	0.0102	0.0306	99.36
183-3-159	52.20	2.10	13.52	10.83	0.19	6.89	11.39	2.03	0.29	0.22	0.0430	0.0123	0.0342	99.73
183-3-193	51.81	2.09	13.36	10.95	0.19	6.87	11.56	2.04	0.29	0.19	0.0467	0.0132	0.0249	99.43
183-3-48	52.21	1.89	13.81	10.25	0.20	6.87	11.59	2.05	0.34	0.21	0.0480	0.0074	0.0310	99.50
183-3-137	52.02	2.11	13.89	10.34	0.20	6.58	11.54	2.21	0.29	0.26	0.1260	0.0085	0.0336	99.62
183-3-95	52.11	2.18	13.60	10.74	0.15	6.51	11.41	2.21	0.28	0.20	0.0480	0.0125	0.0312	99.46
183-3-92	51.83	2.16	13.37	10.93	0.19	6.49	11.76	2.03	0.28	0.19	0.0491	0.0146	0.0320	99.33
183-3-32	51.79	2.13	13.89	10.10	0.17	6.43	11.57	2.22	0.31	0.22	0.1448	0.0095	0.0342	99.02
183-3-129	52.05	2.11	13.62	10.74	0.17	6.35	11.92	2.02	0.28	0.20	0.0409	0.0137	0.0331	99.54
183-3-161	51.98	2.11	13.66	10.91	0.21	6.30	11.96	2.04	0.28	0.23	0.0440	0.0136	0.0403	99.77
183-3-74	51.11	2.13	13.53	11.19	0.19	6.27	11.75	1.93	0.30	0.19	0.1157	0.0084	0.0392	98.76
183-3-133	52.13	2.20	13.86	10.23	0.16	6.25	11.46	2.20	0.34	0.20	0.0450	0.0110	0.0322	99.11
183-3-189	52.02	2.16	13.70	11.10	0.21	6.21	11.69	2.11	0.28	0.18	0.0410	0.0148	0.0357	99.76
183-3-26	51.78	2.23	13.61	10.79	0.18	6.17	11.77	2.06	0.28	0.18	0.0445	0.0131	0.0290	99.13
183-3-53	52.25	2.20	13.78	11.05	0.16	6.12	11.63	2.20	0.29	0.20	0.0413	0.0150	0.0299	99.95
183-3-46	51.25	2.01	13.72	11.04	0.21	5.99	12.63	1.87	0.27	0.21	0.1370	0.0155	0.0308	99.41
183-3-141	52.29	2.17	13.79	10.32	0.17	5.93	11.27	2.23	0.32	0.22	0.1568	0.0089	0.0304	98.92
183-3-77	52.43	2.26	14.20	10.00	0.15	5.93	11.39	2.31	0.38	0.20	0.0548	0.0136	0.0254	99.35
183-3-21a	51.37	2.10	13.28	11.73	0.22	5.91	11.55	2.09	0.28	0.21	0.0248	0.0092	0.0386	98.81
183-3-38	51.63	2.21	13.55	10.80	0.20	5.89	12.05	2.01	0.33	0.18	0.0403	0.0116	0.0285	98.93
183-3-3	51.17	1.96	13.03	12.31	0.24	5.85	11.19	1.95	0.28	0.19	0.0669	0.0083	0.0317	98.28
183-7[a]	52.18	2.15	14.57	7.75	0.16	7.71	11.71	2.08	0.30	0.23	0.1202	0.0092	0.0378	99.02
183-7m	52.09	2.10	13.94	10.22	0.16	7.25	10.93	2.21	0.31	0.18	0.0387	0.0160	0.0304	99.51
183-7-4	51.75	2.00	14.30	10.08	0.18	6.78	11.28	2.14	0.28	0.16	0.0284	0.0121	0.0333	99.08
184-2-3	52.37	2.00	14.36	9.06	0.18	7.33	11.01	2.16	0.41	0.21	0.1406	0.0114	0.0350	99.30
184-5-2[a]	52.58	2.20	14.81	8.17	0.17	6.88	11.50	2.31	0.31	0.18	0.1151	0.0111	0.0354	99.33
184-5-2m	51.83	2.07	14.28	9.91	0.17	6.88	10.91	2.26	0.33	0.21	0.0742	0.0128	0.0323	99.03
184-5-5[a]	53.42	2.24	15.44	7.37	0.20	5.90	12.16	2.06	0.34	0.23	0.1127	0.0111	0.0320	99.53
184-7m	50.83	2.32	14.06	11.91	0.18	6.72	11.12	1.95	0.32	0.21	0.0544	0.0215	0.0410	99.77
184-7-2h[a]	51.98	2.02	13.47	7.98	0.16	9.92	10.94	2.09	0.27	0.18	0.0888	0.0088	0.0543	99.23
184-7-2h	50.83	1.93	13.36	11.02	0.16	9.50	10.17	1.83	0.44	0.21	0.0102	0.0062	0.0060	99.54
184-7-5[a]	57.97	1.38	16.68	6.47	0.23	2.57	11.11	3.24	0.25	0.46	0.0772	0.0068	0.0427	100.48
183-12-4[a]	52.79	2.24	15.36	7.84	0.21	5.84	12.15	2.23	0.32	0.21	0.1087	0.0114	0.0347	99.34
183-12-6m	52.46	2.04	14.15	9.93	0.17	7.30	10.89	2.22	0.31	0.14	0.0211	0.0126	0.0295	99.70
182-8a-1m h[a]	51.02	2.05	13.79	7.57	0.16	11.01	10.72	2.09	0.30	0.25	0.0811	0.0108	0.0304	99.15

Appendix 2 (Contd.)

182-8a-1h[a]	50.85	2.07	13.83	7.79	0.16	11.11	10.70	2.04	0.32	0.23	0.0863	0.0100	0.0329	99.23
182-8b-1	50.51	2.12	13.57	8.79	0.17	10.28	10.79	2.01	0.35	0.25	0.1006	0.0117	0.0299	99.02
182-8b-2h	50.51	2.05	13.32	9.54	0.16	10.30	10.97	1.95	0.33	0.18	0.1024	0.0105	0.0328	99.52
182-8-5[a]	52.73	2.49	15.83	8.56	0.22	3.71	12.98	2.17	0.39	0.25	0.1045	0.0166	0.0346	99.50
183-15-1	54.44	1.90	16.91	9.26	0.24	2.89	10.42	2.53	0.29	0.28	0.1390	0.0118	0.0192	99.31

References

Barnard WM (1995) Mauna Loa Volcano: historical eruptions, exploration, and observations (1779–1910). In: Rhodes JM, Lockwood JP (eds) Mauna Loa revealed: structure, composition, history, and hazards. Am Geophys Union Geophys Monogr 92:1–19

Byers CD, Garcia MO, Muenow DW (1985) Volatiles in pillow rim glasses from Loihi and Kilauea volcanoes, Hawaii. Geochim Cosmochim Acta 49:1887–1896

Carroll MR, Webster JD (1994) Solubilities of sulfur, noble gases, nitrogen, chlorine, and fluorine in magmas. Rev Mineral Volatiles Magmas 30:231–279

Clague DA, Weber WS, Dixon JE (1991) Picritic glasses from Hawaii. Nature 353:553–556

Clague DA, Moore JG, Dixon JE, Friesen WB (1995) Petrology of submarine lavas from Kilauea's Puna Ridge, Hawaii. J Petrol 36:299–349

Danyushevsky LV, Della-Pasqua FN, Sokolov S (2000) Re-equilibrium of melt inclusions trapped by magnesian olivine phenocrysts from subduction-related magmas: petrological implications. Contrib Mineral Petrol 138:68–83

Decker RW, Koyanagi RY, Dvorak JJ, Lockwood JP, Okamura AT, Yamashita KM, Tanigawa WR (1983) Seismicity and surface deformation of Mauna Loa Volcano, Hawaii. EOS Trans Am Geophys Union 64:545–547

DePaolo DJ, Bryce JG, Dodson A, Shuster, DL, Kennedy BM (2001) Isotopic evolution of Mauna Loa and the chemical structure of the Hawaiian plume. Geochem Geophys Geosci 3:2000GC000139

Dixon JE, Clague DA (2001) Volatiles in basaltic glasses from Loihi Seamount: evidence for a relatively dry plume source. J Petrol 42:627–654

Dixon JE, Pan V (1995) Determination of molar absorptivity of dissolved carbonate in basanitic glass. Am Mineral 80:1339–1342

Dixon JE, Stolper EM (1995) An experimental study of water and carbon dioxide solubilities in mid-ocean ridge basaltic liquids. Part II: application to degassing of basaltic liquids. J Petrol 36:1633–1646

Dixon JE, Clague DA, Stolper EM (1991) Degassing history of water, sulfur, and carbon in submarine lavas from Kilauea Volcano, Hawaii. J Geol 99:371–394

Dixon JE, Stolper EM, Holloway JR (1995) An experimental study of water and carbon dioxide solubilities in mid-ocean ridge basaltic liquids. Part I: calibration and solubility models. J Petrol 36:1607–1631

Fine G, Stolper E (1986) Carbon dioxide in basaltic glasses: concentrations and speciation. Earth Planet Sci Lett 76:263–278

Fornari DJ, Malahoff A, Heezen BC (1979a) Submarine slope micromorphology and volcanic substructure of the island of Hawaii inferred from visual observations made from US Navy deep-submergence vehicle (DSV) *Sea Cliff*. Mar Geol 32:1–20

Fornari DJ, Peterson DW, Lockwood JP, Malahoff A, Heezen BC (1979b) Submarine extension of the southwest rift zone of Mauna Loa Volcano, Hawaii: visual observations from US Navy Deep submergence vehicle DSV *Sea Cliff*. Geol Soc Am Bull 90:435–443

Fornari DJ, Lockwood JP, Lipman PW, Rawson M, Malahoff A (1980) Submarine volcanic features west of Kealakekua Bay, Hawaii. J Volcanol Geotherm Res 7:323–337

Gaetani GA, Watson EB (2000) Open system behavior of olivine-hosted melt inclusions. Earth Planet Sci Lett 183:27–41

Garcia MO (1996) Petrography and olivine and glass chemistry of lavas from the Hawaii Scientific Drilling Project. J Geophys Res 101:11701–11713

Garcia MO, Davis MG (2001) Submarine growth and internal structure of oceanic island volcanoes based on submarine observations of Mauna Loa Volcano, Hawaii. Geology 29:163–166

Garcia MO, Muenow DW, Aggrey KE, O'Neil JR (1989) Major element, volatile, and stable isotope geochemistry of Hawaiian submarine tholeiitic glasses. J Geophys Res 94:10525–10538

Garcia MO, Foss DJP, West HB, Mahoney JJ (1995a) Geochemical and isotopic evolution of Loihi Volcano, Hawaii. J Petrol 36:1647–1674

Garcia MO, Hulsebosch TP, Rhodes JM (1995b) Olivine-rich submarine basalts from the southwest rift zone of Mauna Loa Volcano: implications for magmatic processes and geochemical evolution. In: Rhodes JM, Lockwood JP (eds) Mauna Loa revealed: structure, composition, history, and hazards. Am Geophys Union Geophys Monogr 92:219–239

Garcia MO, Pietruszka AJ, Rhodes JM, Swanson K (2000) Magmatic processes during the prolonged Puu Oo eruption of Kilauea Volcano, Hawaii. J Petrol 41:967–990

Gerlach TM (1993) Oxygen buffering of Kilauea volcanic gases and the oxygen fugacity of Kilauea basalt. Geochim Cosmochim Acta 57:795–814

Gerlach TM, Graeber EJ (1985) Volatile budget of Kilauea Volcano. Nature 313:273–277

Ghiorso MS, Sack RO (1995) Chemical mass transfer in magmatic processes IV: a revised and internally consistent thermodynamic model for interpolation and extrapolation. Contrib Mineral Petrol 119:197–212

Greenland LP (1987a) Hawaiian eruptive gases. Volcanism in Hawaii. US Geol Surv Prof Pap 1350, pp 759–770

Greenland LP (1987b) Composition of gases from the 1984 eruption of Mauna Loa Volcano. Volcanism in Hawaii. US Geol Surv Prof Pap 1350, pp 781–790

Gurriet PC (1988) Geochemistry of Hawaiian dredged lavas. MSc Thesis, Massachusetts Institute of Technology

Hauri E (1996) Major element variability in the Hawaiian mantle plume. Nature 382:415–419

Hauri E (2002) SIMS analysis of volatiles in silicate glasses, 2: isotopes and abundances in Hawaiian melt inclusion. Chem Geol 183:115–141

Hein JR, Gibbs AE, Clague DA, Torresan M (1996) Hydrothermal mineralization along submarine rift zones, Hawaii. Mar Geores Geotech 14:177–203

Hill DP, Zucca JJ (1987) Geophysical constraints on the structure of Kilauea and Mauna Loa Volcanoes and some implications for seismomagmatic processes. Volcanism in Hawaii. US Geol Surv Prof Pap 1350, pp 903–917

Jaggar TA (1940) Magmatic gases. Am J Sci 238:313–353

Jaggar TA (1947) Origin and evolution of craters. Geol Soc Am Mem vol 121

Jarosewich E, Nelson JA, Norberg JA (1979) Electron microprobe reference samples for mineral analyses. Smithsonian Contrib Earth Sci 22:68–72

Johnson DJ (1995) Gravity changes on Mauna Loa Volcano. In: Rhodes JM, Lockwood JP (eds) Mauna Loa revealed: structure, composition, history, and hazards. Am Geophys Union Geophys Monogr 92:127–143
Kahle AB, Abrams MJ, Abbott EA, Mouginis-Mark PJ, Realmuto VJ (1995) Remote sensing of Mauna Loa. In: Rhodes JM, Lockwood JP (eds) Mauna Loa revealed: structure, composition, history, and hazards. Am Geophys Union Geophys Monogr 92:145–170
Kamenetsky V, Clocchiatti R (1996) Primitive magmatism of Mt. Etna: insights from mineralogy and melt inclusions. Earth Planet Sci Lett 142:553–572
Kent AJR, Clague DA, Honda M, Stolper EM, Hutcheon ID, Norman MD (1999a) Widespread assimilation of a seawater-derived component at Loihi Seamount, Hawaii. Geochim Cosmochim Acta 63:2749–2761
Kent AJR, Norman MD, Hutcheon ID, Stolper EM (1999b) Assimilation of seawater-derived components in an oceanic volcano: evidence from matrix glasses and glass inclusions from Loihi seamount, Hawaii. Chem Geol 156:299–319
Kurz MD, Kenna TC, Kammer DP, Rhodes JM, Garcia MO (1995) Isotopic evolution of Mauna Loa Volcano: a view from the submarine southwest rift zone. In: Rhodes JM, Lockwood JP (eds) Mauna Loa revealed: structure, composition, history, and hazards. Am Geophys Union Geophys Monogr 92:289–306
Lange RA (1994) The Effect of H_2O, CO_2 and F on the density and viscosity of silicate melts. Rev Mineral Volatiles Magmas 30:331–369
Langmuir CH (1989) Geochemical consequences of in situ crystallization. Nature 340:199–205
Lipman PW, Normark WR, Moore JG, Wilson JB, Gutmacher CE (1988) The giant submarine Alika debris slide, Mauna Loa, Hawaii. J Geophys Res 93:4279–4299
Lipman PW, Rhodes JM, Dalrymple GB (1990) The Ninole Basalt – implications for the structural evolution of Mauna Loa Volcano, Hawaii. Bull Volcanol 53:1–19
Lockwood JP, Lipman PW, Petersen LD, Warshauer FR (1988) Generalized ages of surface lava flows of Mauna Loa Volcano, Hawaii. US Geol Survey Misc Invest Map I-1908
Mathez EA (1976) Sulfur solubility and magmatic sulfides in submarine basalt glass. J Geophys Res 81:4269–4276
Michael PJ, Cornell WC (1998) Influence of spreading rate and magma supply on crystallization and assimilation beneath mid-ocean ridges: evidence from chlorine and major element chemistry of mid-ocean ridge basalts. J Geophys Res 103:18325–18356
Michael PJ, Schilling J-G (1989) Chlorine in mid-ocean ridge magmas: evidence for assimilation of seawater-influenced components. Geochim Cosmochim Acta 53:3131–3143
Montierth C, Johnston AD, Cashman KV (1995) An empirical glass-composition-based geothermometer for Mauna Loa lavas. In: Rhodes JM, Lockwood JP (eds) Mauna Loa revealed: structure, composition, history, and hazards. Am Geophys Union Geophys Monogr 92:207–217
Moore JG (1965) Petrology of deep-sea basalt near Hawaii. Am J Sci 263:40–521
Moore JG (1970) Water content of basalt erupted on the ocean floor. Contrib Mineral Petrol 28:272–279
Moore JG, Chadwick WW (1995) Offshore geology of Mauna Loa and adjacent areas, Hawaii. In: Rhodes JM, Lockwood JP (eds) Mauna Loa revealed: structure, composition, history, and hazards. Am Geophys Union Geophys Monogr 92:21–44
Moore JG, Clague DA (1992) Volcano growth and evolution of the island of Hawaii. Geol Soc Am Bull 104:1471–1484
Moore JG, Fabbi BP (1971) An estimate of the juvenile sulfur content of basalt. Contrib Mineral Petrol 33:118–127
Moore JG, Fiske RS (1969) Volcanic substructure inferred from dredge samples and ocean-bottom photographs, Hawaii. Geol Soc Am Bull 80:1191–1201
Moore JG, Fornari DJ, Clague DA (1985) Basalts from the 1877 submarine eruption of Mauna Loa, Hawaii: new data on the variation of palagonitization rate with temperature. US Geol Surv Bull 1663:1–11
Moore JG, Clague DA, Holcomb RT, Lipman PW, Normark WR, Torresan ME (1989) Prodigious submarine landslides on the Hawaiian Ridge. J Geophys Res 94:17465–17484
Moore JG, Normark WR, Szabo BJ (1990) Reef growth and volcanism on the submarine southwest rift zone of Mauna Loa, Hawaii. Bull Volcanol 52:375–380
Moore JG, Normark WR, Holcomb RT (1994) Giant Hawaiian landslides. Annu Rev Earth Planet Sci 22:119–144
Moore JG, Bryan WB, Beeson MH, Normark WR (1995) Giant blocks in the South Kona landslide, Hawaii. Geology 23:125–128
Muenow DW, Graham DG, Liu N, Delaney JR (1979) The abundance of volatiles in Hawaiian tholeiitic submarine basalts. Earth Planet Sci Lett 42:71–76
Naughton JJ, Finlayson JB, Lewis VA (1975) Some results from recent chemical studies at Kilauea Volcano, Hawaii. Bull Volcanol 39:64–69
O'Hara MJ, Matthews RE (1981) Geochemical evolution in an advancing, periodically replenished, periodically tapped, continuously fractionated magma chamber. J Geol Soc Lond 138:237–277
Okubo PG (1995) A seismological framework for Mauna Loa Volcano, Hawaii. In: Rhodes JM, Lockwood JP (eds) Mauna Loa revealed: structure, composition, history, and hazards. Am Geophys Union Geophys Monogr 92:187–197
Oskarsson N (1980) The interaction between volcanic gases and tephra: fluorine adhering to tephra of the 1970 Hekla eruption. J Volcanol Geotherm Res 8:251–266
Rampino MR, Self S, Stothers RB (1988) Volcanic winters. Ann Rev Earth Planet Sci 16:73–99
Rhodes JM (1988) Geochemistry of the 1984 Mauna Loa eruption: implications for magma storage and supply. J Geophys Res 93:4453–4466
Rhodes JM (1995) The 1852 and 1868 Mauna Loa picrite eruptions: clues to parental magma compositions and the magmatic plumbing system. In: Rhodes JM, Lockwood JP (eds) Mauna Loa revealed: structure, composition, history, and hazards. Am Geophys Union Geophys Monogr 92:241–262
Rhodes JM, Hart SR (1995) Episodic trace element and isotopic variations in historical Mauna Loa lavas: implications for magma and plume dynamics. In: Rhodes JM, Lockwood JP (eds) Mauna Loa revealed: structure, composition, history, and hazards. Am Geophys Union Geophys Monogr 92:263–288
Richter DH, Eaton JP, Murata KJ Ault WU, Krivoy HL (1970) Chronology narrative of the 1959–1960 eruption of Kilauea Volcano, Hawaii. US Geol Surv Prof Paper 537-E
Robinson BW, Graham J (1982) Advances in electron microprobe trace element analysis. J Computer Assist Microsci 4:263–265
Roedder E (1979) Origin and significance of magmatic inclusions. Bull Mineral 102:487–510
Rowe EC, Schilling JG (1979) Fluorine in Iceland and Reykjanes Ridge basalts. Nature 279:33–37
Ryan S (1995) Quiescent outgassing of Mauna Loa Volcano 1958–1994. In: Rhodes JM, Lockwood JP (eds) Mauna Loa revealed: structure, composition, history, and hazards. Am Geophys Union Geophys Monogr 92:95–115
Sigvaldason GE, Oskarsson N (1986) Fluorine in basalts from Iceland. Contrib Mineral Petrol 94:263–271
Sobolev AV, Hofmann AW, Nikogosian IK (2000) Recycled oceanic crust observed in ''ghost plagioclase'' within the source of Mauna Loa lavas. Nature 247:986–990
Stebbins JF, Zeng Q (2000) Cation ordering at fluoride sites in silicate glasses: a high resolution 19F NMR study. J Non-Crystal Solids 262:1–5
Swanson DA, Fabbi BP (1973) Loss of volatiles during fountaining and flowage of basaltic lava at Kilauea Volcano, Hawaii. J Res US Geol Surv 1:649–658
Thordarson T, Self S, Oskarsson N, Hulsebosch T (1996) Sulfur, chlorine, and fluorine degassing and atmospheric loading by the

1783–1784 A.D. Laki (Skaftar Fires) eruption in Iceland. Bull Volcanol 58:205–225

Todd CS (1996) Fluorine analysis by electron microprobe: correction for iron interference. Geol Soc Am Abstr 28(7):212

Tribble GW (1991) Underwater observations of active lava flows from Kilauea Volcano, Hawaii. Geology 19:633–636

Trusdell FA (1995) Lava flow hazards and risk assessment on Mauna Loa Volcano, Hawaii. In: Rhodes JM, Lockwood JP (eds) Mauna Loa revealed: structure, composition, history, and hazards. Am Geophys Union Geophys Monogr 92:327–336

Unni CK, Schilling J-G (1978) Cl and Br degassing by volcanism along the Reykjanes Ridge and Iceland. Nature 272:19–23

Wallace PJ (2002) Volatiles in submarine basaltic glasses from the Northern Kerguelen Plateau (ODP Site 1140): implications for source region compositions, shallow magmatic processes, and plateau subsidence. J Petrol 43:1311–1326

Wallace PJ, Anderson AT Jr (1998) Effects of eruption and lava drainback on the H_2O contents of basaltic magmas at Kilauea Volcano. Bull Volcanol 59:327–344

Wallace PJ, Carmichael ISE (1992) Sulfur in basaltic magmas. Geochim Cosmochim Acta 56:1863–1874

Wallace PJ, Carmichael ISE (1994) S speciation in submarine basaltic glasses as determined by measurements of SKα X-ray wavelength shifts. Am Mineral 79:161–167

Wolfe EW, Morris J (1996) Geologic map of the island of Hawaii. US Geol Surv Misc Invest Map I-2524

Yi W, Halliday AN, Alt JC, Lee D-C, Rehkamper M, Garcia MO, Langmuir CH, Su Y (2000) Cadmium, indium, tin, tellurium and sulfur in oceanic basalts: implications for chalcophile element fractionation in the mantle. J Geophys Res 105:18927–18948